Pergamon

Geochimica et Cosmochimica Acta, Vol. 65, No. 16, pp. 2651–2668, 2001

0016-7037/01 $20.00 + .00

PII S0016-7037(01)00618-4

Fluid inclusion noble gas and halogen evidence on the origin of Cu-Porphyry mineralising fluids

M. A. KENDRICK, R. BURGESS,* R. A. D. PATTRICK, and G. TURNER

[1]Department of Earth Sciences, University of Manchester, Oxford Rd., Manchester, M13 9PL, U.K.

(*Received September* 29, 2000; *accepted in revised form March* 19, 2001)

Abstract—The naturally occurring noble gas isotopes (^{40}Ar, ^{36}Ar, ^{84}Kr and ^{129}Xe) and halogens (Cl, Br, I) have been determined simultaneously in irradiated quartz vein samples by noble gas mass spectrometry. Quartz vein samples were collected from the potassic and propylitic alteration zones of six porphyry copper deposits (PCD): Bingham Canyon, Utah; and Silverbell, Ray, Mission, Pinto Valley and Globe-Miami in Arizona. In addition, analyses of ^{3}He/^{4}He have been obtained from sulphide minerals hosted by the quartz veins at Silverbell, Ray, Pinto Valley and Globe-Miami.

The majority of PCD fluids studied have Br/Cl and I/Cl ratios that overlap those of fluids included in mantle diamond, suggesting that the salinity had a juvenile origin. The high I/Cl (121×10^{-6} mole, M) in samples from the propylitic zone of Silverbell is attributed to the presence of sedimentary formation water.

^{3}He/^{4}He ratios have R/Ra values in the range 0.3 to 1.72, and provide evidence for the involvement of a crustal component in addition to mantle volatiles. ^{40}Ar/^{36}Ar ratios vary from meteoric values of ~317 in the propylitic zone of Bingham Canyon, and 323 in the skarn alteration of Mission up to 3225 in the potassic zone of Pinto Valley. Fluids in both the potassic and propylitic alteration zones of every deposit are a mixture of a low salinity end-member comprising meteoric water and air, and a high salinity end-member consisting of a mixed mantle and crustal fluid.

The ^{40}Ar/Cl ratio of fluid inclusions at Pinto Valley ($\sim 10^{-4}$ M) is similar to values obtained previously for mantle fluids. The ^{40}Ar/Cl value is two orders of magnitude lower at Bingham Canyon, where a depleted ^{36}Ar concentration (0.2×10^{-6} cm^3/g) below that of air saturated water (ASW), and a range of highly fractionated noble gas compositions ($F^{84}Kr = 13$ and $F^{129}Xe = 160$) indicate that boiling and pulsed fluid flow have occurred. *Copyright © 2001 Elsevier Science Ltd*

1. INTRODUCTION

Saline fluids are arguably the most important mineralising component in hydrothermal systems and the combined study of noble gases and halogens can be used to determine the origin of the fluid, the source of salinity and the age of mineralisation. Fluids of different origins (meteoric, magmatic or sedimentary formation water) have characteristic noble gas isotope signatures, and noble gases can be used to quantitatively evaluate the contribution of these different components to a hydrothermal fluid (e.g., Turner et al., 1993). Hydrothermal fluids may attain a high salinity by a number of mechanisms including, partitioning of juvenile halogens into a magmatic fluid phase, boiling, dissolution of evaporites, and evaporation of seawater. These processes can be resolved because they lead to characteristic halogen signatures (Bohlke and Irwin, 1992a; Worden, 1996).

Extension of the Ar-Ar technique allows simultaneous determination of the halogens (Cl, Br, I), and the naturally occurring noble gas isotopes of Ar, Kr, and Xe, by noble gas mass spectrometry (Kelley et al., 1986; Bohlke and Irwin, 1992b). In addition to information on fluid origins, the technique can, under the right circumstances, provide direct age determinations (Kelley et al., 1986; Turner and Bannon, 1992; Kendrick et al., 2001).

Combined noble gas and halogen analysis has been applied to a variety of hydrothermal systems, and has provided an overview to geothermal, metamorphic, Mississippi Valley-Type and granite related systems (Kelley et al., 1986; Bohlke and Irwin, 1992a; Bohlke and Irwin, 1992c; Turner and Bannon, 1992; Burgess and Parsons, 1994; Irwin and Reynolds, 1995; Irwin and Roedder, 1995). Of the granite related hydrothermal systems, two porphyry copper deposits have been investigated: Bingham Canyon, Utah, and Butte, Montana, both in the USA (Irwin and Roedder, 1995).

The present work focuses on the origin of fluids associated with porphyry copper deposit (PCD) mineralisation. Detailed study of the noble gas and halogen composition of fluids involved in PCD genesis will test their uniformity and origin. Heavy noble gas (Ar, Kr and Xe) and halogen analysis of irradiated quartz vein samples and helium isotope analyses of associated unirradiated sulphides have been undertaken. Ar-Ar age determinations made possible through this work have provided the focus to a separate publication (Kendrick et al., 2001).

1.1. Porphyry Copper Deposits

PCD fluids have been well characterised by both fluid inclusion and stable isotope studies. Classic studies include: Roedder (1971; 1984); Sheppard et al. (1971); Nash (1976); Sheppard and Gustafson (1976); Eastoe (1978); Beane and Titley (1981) and Bowman et al. (1987). The abundant data available from conventional techniques enables a comparison with infor-

*Author to whom correspondence should be addressed (Ray.Burgess@man.ac.uk).

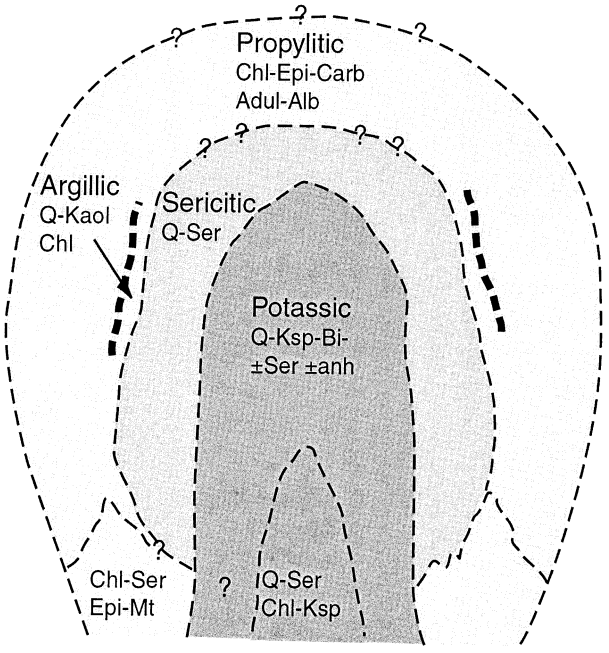

Fig. 1. Schematic drawing of alteration zoning in a typical porphyry copper deposit (after Guilbert and Lowell, 1974). Samples in this study come from the potassic and propylitic zones (Table 1). Q = quartz; Ksp = K-feldspar; Bi = biotite; Ser = Sericite; anh = anhydrite; Chl = chlorite; Epi = epidote; Carb = carbonate; Adul = adularia; Alb = albite; Kaol = kaolinite; mt = magnetite.

mation obtained through combined noble gas and halogen analysis.

PCD wall rock alteration is genetically related to and centred upon, an evolved calc-alkaline porphyritic stock (Fig. 1). Fluid inclusion data shows that 'magmatic' fluids of the inner potassic zone have temperatures up to 725°C and salinities as high as 60 wt.% NaCl equ. (Roedder, 1984). The outer propylitic zone fluids have lower temperature and salinity, e.g., at Bingham Canyon approximately 370°C and 33 wt % NaCl equ. (Bowman et al., 1987). Fluid inclusions in the temporally later sericitic and argillic alteration zones yield lower fluid inclusion homogenisation temperatures and lower salinities (3–20 wt.% NaCl equ.), compatible with the system becoming invaded and progressively dominated by meteoric water.

Comparison between different PCD deposits reveals that the stable isotope (O and H) composition of potassic zone biotites is independent of latitude, and overlaps that of a hypothetical primary magmatic composition (see Taylor, 1997). In contrast, the stable isotope composition of clay and sericite from the later sericitic/argillic alteration zones are dependent on latitude, supporting the predominance of external meteoric or sedimentary formation water in the outer/later zones (Sheppard et al., 1969; Sheppard et al., 1971; Sheppard and Taylor, 1974).

At individual deposits stable isotope data can be less conclusive in that it is difficult to distinguish isotopically modified meteoric water from sedimentary formation water. For example at Bingham Canyon the composition of propylitic zone fluids can be explained by either mixing of magmatic and D-enriched formation water, or by isotopic exchange between meteoric water and igneous rocks at very low water/rock ratio (Bowman et al., 1987). Unmodified meteoric fluids may have been important in only the late sericitic and argillic alteration zones. The importance of sedimentary formation waters has also been demonstrated at the Ann-Mason deposit, Yerington, Nevada (Dilles et al., 1992).

The PCD deposits chosen in this study are the 5Gt Bingham Canyon deposit, Utah, USA (Moore and Nash, 1974; Lanier et al., 1978; Warnaars et al., 1978; Bowman et al., 1987; Irwin and Roedder, 1995) and five smaller deposits from the Laramide metallogenic province in southwest Arizona, USA. The Arizonan deposits include; Silverbell, Ray, Pinto Valley, Globe-Miami and Mission (e.g., Livingston, 1973; Nash, 1976; Titley, 1982; 1994; 1995; Titley et al., 1989). Although all the deposits show the classic features of PCD mineralisation, alteration styles at the six deposits vary (Table 1), providing the opportunity to compare common features of fluid evolution as well as the extent of noble gas and halogen variation

1.2. Noble Gases and Halogens in Crustal Fluids

The noble gases are chemically inert, and show conservative behaviour in the Earth's crust. The abundance of the noble gases Ar, Kr, and Xe in a fluid and their ratios to each other, particularly an atmospheric $^{40}Ar/^{36}Ar$ ratio of 295.5, can determine whether a fluid originated at the surface. Furthermore, the temperature and salinity dependence of noble gas solubility (Smith and Kennedy, 1983) means that in principle, meteoric water and seawater can be distinguished using noble gas concentration data (Bohlke and Irwin, 1992c). $^{40}Ar/^{36}Ar$ ratios above the atmospheric value of 295.5 indicate enrichment of the fluid in excess ^{40}Ar ($^{40}Ar_E$) from either a crustal or mantle source. $^{40}Ar_E$ is the ^{40}Ar not attributable to an atmospheric origin or to in situ production from radioactive decay of ^{40}K. A crustal fluid may acquire $^{40}Ar_E$ by interaction with K-rich rocks, or from degassing of the upper mantle, which has $^{40}Ar/^{36}Ar > 40\,000$ (e.g., Burnard et al., 1997). An upper mantle noble gas component is most easily recognised by having a high $^3He/^4He$ (R) value of ~8 Ra (Ra = the atmospheric value of 1.4×10^{-6}), and is therefore distinct from a typical crustal He signature of between 0.01 and 0.05 Ra (Tolstikhin, 1978; O'Nions and Oxburgh, 1988).

The evolution of a fluid in the crust may involve changes of state, such as boiling, which leads to fractionation of noble gases (Ar, Kr, Xe) and Cl, but does not affect the noble gas isotope signatures (e.g., $^{40}Ar/^{36}Ar$). When such a fractionation occurs the residual fluid will become enriched in Cl and depleted in the noble gases which are partitioned overwhelmingly into the vapour phase. However, in relative terms the residue will exhibit an enrichment in the less volatile heavier noble gases (Xe>Kr>Ar) and the vapour phase will be enriched in the lighter more volatile noble gases (Ar>Kr>Xe) making identification of such a process relatively straight forward.

The use of halogens as conservative fluid tracers and indicators of the acquisition of salinity has been demonstrated through Br/Cl studies of sedimentary brines (e.g., Crocetti and Holland, 1989; Viets et al., 1996; Worden, 1996). Analysis of iodine, which is usually the least abundant halogen in fluid inclusions, is possible because of the high sensitivity of the noble gas neutron activation technique. In the present study, the determination of I/Cl in addition to Br/Cl has enabled the

Table 1 Summary of deposit characteristics and samples

Deposit features				Sample features		Fluid inclusion frequency			
Host rocks	Mineralisation style at deposit	Age (Ma)	Ref[a]	Sample	Vein	LV	V	LVD	Average salinity[b]
Bingham Canyon									
Bingham stock is the major host, comprising quartz monzonite and latite porphyry dykes.	K-silicate, minor skarn alteration. Pyrite rich outer zones.	c.39	[1]	BC5-A	5cm wide molybdenite bearing quartz vein, with minor chalcopyrite. Central potassic zone	High	High	High	17%
		37.1 ± 0.5	[2]	BC5-B					
			[3]	BC5-C					
Mineralisation is also found in the Jordan and Commercial Limestone beds of the Bingham Mine Fm.			[10]	BC4	Quartz vein (~1 cm) hosted by highly altered monozonite; potasic zone, with a late sericitic overprint.	High	High	Low	14%
				BC3	Chalcopyrite and molybdenite bearing quartz veinlets hosted by potassically altered monzonite.	High	High	Low	14%
				BC2	Quartz veinlet through equigranular monzonite of the propylitic zone. Associated with pyrite stringers.	v. High	Rare	Zero	2%
Mission									
90-95% of mineralisation is in sediments, mostly carbonate dominated Palaeozoic rocks. In the Epitaph Fm. gypsiferous units are significant.	Dominantly skarn alteration, including a variety of skarn types.	c.58	[4] [5]	M3	Skarn hosted chalcopyrite bearing quartz vein from the garnet wollastonite tactite zone.	v. High	Low	Zero	4%
Ray									
Mafic diabase sills are the most important host. Precambrian rocks; Pinal Schist and Apache Group sediments are also present. Laramide igneous rocks are unimportant in the area.	K-silicate; biotite replaces K-feldspar as the dominant alteration mineral. Intense late stage quartz sericite alteration is common.	60.8–70.5	[5]	R1	Pyrite bearing quartz vein hosted by potasically altered Granite Mountian Porphyry.	v. High	Rare	Rare	10%
		65.4	[6]						
		65.3 ± 1.5	[7] [10]	R3	Pyrite bearing quartz vein hosted by propylytically altered Pinal Schist.	v. High	None	None	5%
Pinto Valley/Globe Miami									
The Schultze Granite, and Precambrian wall rocks; Pinal Schists and granites. Also the Apache Group sediments and some diabase sills.	K-silicate alteration with intense late stage quartz sericite overprinting.	61.1 ± 0.3	[5]	GM3	Chalcopyrite and pyrite bearing quartz vein. Potassic zone, Bluebird Live Oak Pit.	High	Mod.	Low	10%
		59.5 ± 0.3	[9]						
		59.1 ± 0.5	[10]	GM4	Pyrite bearing quartz vein, taken from the propylitic zone. Intermediate with the potassic zone.	v. High	None	Rare	6%
		61.7 ± 3.4							
		63.2 ± 8.0		PV6	Chalcopyrite bearing quartz vein from ore zone. Hosted by potassically altered quartz monzonite.	v. High	Low	Low	12%
				PV1	Pyrite-bearing quartz vein, phyllic vein selvage. Hosted by Precambrain Gulch Granite.	v. High	Low	Rare	5%
Silverbell									
Large variety of host rocks explain the complex alteration. Palaeozoic sediments and Laramide volcanics, clastics, and andesitic to rhyolitic volcanic flows and intrusions.	K-silicate and skarn alteration. Hypogene Cu ores are low grade 0.05–0.1%.	56–70	[5]	SB4	Pyrite bearing quartz vein hosted by potassically altered alaskite.	v. High	None	None	11%
		65.5 ± 2	[4]						
		55.8 ± 1.8	[8] [10]	SB1	Pyrite and chalococite bearing quartz vein from central monzonite, potassic zone.				
				SB8	Quartz vein from dacite in outer propylitic zone.				
				SB6	Quartz vein from outside edge of monzonite, propylitic zone.	High (2°)	None	None	5%

[a] References: [1]-Warnaars et al. (1978); [2]-Bowman et al. (1987); [3]-Moore and Nash (1974); [4]-Livingston (1973); [5]-Titley et al. (1989); [6]-Banks et al. (1972); [7]-Phillips et al. (1974); [8]-Richard and Courtright, (1966); [9]-Creasey (1980); [10]-Kendrick et al (2001).

[b] Average fluid inclusion salinities expressed as wt. % NaCl equ., are based on thermometric study and the relative abundance of the fluid inclusion types; LV-liquid vapour, V-vapour dominated and LVD-liquid vapour and a daughter mineral. 2° = secondary fluid inclusions common.

Table 2. Summary of noble gas and halogen data

	Quartz[b]						Sulphide[c]			
Sample[a]	$^{40}Ar/^{36}Ar$	$Cl/^{36}Ar$ ($\times 10^6$	$^{40}Ar_E/Cl$	$^{84}Kr/^{36}Ar$ ($\times 10^{-3}$)	Br/Cl ($\times 10^{-3}$)	I/Cl ($\times 10^{-6}$)	$^{40}Ar/^{36}Ar$	$^3He/^4He$ (R/Ra)	$^{40}Ar*/^4He$ ($\times 10^{-3}$)	F^4He
BC5-A	1137 ± 6742	116.8 ± 17.3	3.6×10^{-6}	263.7 ± 39.5	1.23 ± 0.02	16.29 ± 0.71	—	—	—	—
BC5-B	552 ± 64	241.9 ± 98.2	1.4×10^{-6}	38.4 ± 15.6	1.33 ± 0.03	21.38 ± 0.56	—	—	—	—
BC5-C	1894 ± 390	365.3 ± 75.4	3.6×10^{-6}	44.2 ± 9.5	1.05 ± 0.02	18.70 ± 0.47	—	—	—	—
BC4	1222 ± 258	90.8 ± 19.2	8.1×10^{-6}	57.9 ± 3.5	1.54 ± 0.01	21.61 ± 0.22	—	—	—	—
BC3	594 ± 116	66.3 ± 12.9	6.5×10^{-6}	34.9 ± 6.3	1.87 ± 0.01	28.30 ± 0.62	—	—	—	—
BC2	317 ± 5	5.0 ± 0.3	1.2×10^{-5}	28.5 ± 0.4	1.17 ± 0.01	—	—	—	—	—
R1	677 ± 34	37.7 ± 8.2	1.1×10^{-5}	28.0 ± 0.02	0.87 ± 0.01	9.34 ± 0.23	547 ± 3	1.38 ± 0.06	1800 ± 3	870 ± 4
R3	433 ± 12	3.4 ± 0.1	4.7×10^{-5}	29.8 ± 0.02	0.91 ± 0.01	18.38 ± 0.53	813 ± 2	1.72 ± 0.01	970 ± 1	3200 ± 7
GM3	824 ± 41	8.9 ± 0.5	5.7×10^{-5}	28.1 ± 1.4	1.01 ± 0.01	35.63 ± 1.00	907 ± 1	0.32 ± 0.01	370 ± 0	10000 ± 12
GM3	—	—	—	—	—	—	845 ± 22	0.60 ± 0.02	610 ± 1	4700 ± 123
GM4	662 ± 62	29.8 ± 2.8	1.9×10^{-5}	33.1 ± 3.1	1.00 ± 0.04	16.03 ± 0.38	612	0.69	—	—
PV6	3211 ± 920	11.6 ± 3.3	2.7×10^{-4}	41.9 ± 12.0	1.06 ± 0.01	28.54 ± 0.55	670 ± 4	0.62 ± 0.03	1000 ± 1	2200 ± 13
PV6	—	—	—	—	—	—	1063 ± 5	0.76 ± 0.02	1300 ± 2	3500 ± 16
PV1	985 ± 101	4.8 ± 0.5	1.4×10^{-4}	23.9 ± 1.3	1.37 ± 0.02	24.48 ± 0.88	603 ± 2	1.15 ± 0.03	1100 ± 2	1500 ± 5
SB4	372 ± 7	5.4 ± 0.2	1.7×10^{-5}	20.5 ± 0.9	1.23 ± 0.01	99.00 ± 1.92	852 ± 6	1.20 ± 0.01	690 ± 1	4900 ± 36
SB1(5)	324 ± 17	2.5 ± 0.1	1.3×10^{-5}	21.0 ± 1.1	1.24 ± 0.02	69.20 ± 3.77	914 ± 3	1.12 ± 0.01	700 ± 1	5300 ± 15
SB8	1112 ± 114	27.3 ± 2.8	3.3×10^{-5}	35.3 ± 4.3	1.45 ± 0.01	121.00 ± 2.42	—	—	—	—
SB6	609 ± 92	18.9 ± 2.9	1.7×10^{-5}	25.6 ± 2.2	1.58 ± 0.02	89.30 ± 1.53	924 ± 2	0.84 ± 0.02	590 ± 1	5600 ± 13
M3	323 ± 35	8.0 ± 0.9	3.7×10^{-6}	25.7 ± 0.5	0.94 ± 0.01	42.20 ± 2.31	—	—	—	—

[a] Potassic zone samples are in regular font, outer zone samples (mainly propylitic, see Table 1 for details) are in *italic*, Bingham Canyon (BC), Ray (R), Globe-Miami (GM), Pinto Valley (PV), Silverbell (SB) and Mission (M).

[b] The noble gas ratios ($^{40}Ar/^{36}Ar$, $Cl/^{36}Ar$ and $^{84}Kr/^{36}Ar$) are the highest values determined during sequential *in vacuo* crushing; usually the first or second crushing extraction. They are considered to be the analyses most free of air contamination and therefore representative of the magmatic fluid end-member. The $^{40}Ar_E/Cl$ ratio is obtained from linear correlation between $^{40}Ar/^{36}Ar$ and $Cl/^{36}Ar$ (shown in Fig 4). The halogen compositions are obtained by summing the gas released during both in vacuo crushing and step heating experiments (Kendrick et al. 2001).

[c] The noble gas composition of fluids included in sulphide were determined by a single in vacuo crushing experiment of ~1g sample. F^4He values reflect enrichment of ^4He in the fluid relative to air; $F^4He = (^4He/^{36}Ar)_{sample}/(^4He/^{36}Ar)_{air}$ where $^4He/^{36}Ar_{air} = 0.1655$.

composition of a 'juvenile' magmatic signature to be confidently resolved from that of evolved seawater and sedimentary formation water.

2. EXPERIMENTAL METHODS AND SAMPLING

Quartz vein samples have been collected from the central potassic and outer alteration zones of the following porphyry copper deposits; Bingham Canyon (BC), Utah, and Silverbell (SB), Globe-Miami (GM), Pinto Valley (PV) and Ray (R), in Arizona, as well as from skarn alteration at Mission (M), Arizona. Before noble gas analysis, characterisation of fluid inclusion populations and limited thermometric determinations enabled average salinities to be estimated (Table 1). Samples were crushed, and quartz chips (1–3mm size, total 60–90 mg) were hand-picked under a binocular microscope and cleaned in an ultrasonic bath using distilled water and acetone. Three samples were selected from a single 5cm wide vein at Bingham Canyon (BC5- A, B and C) to detect any localised variations in fluid composition.

Quartz vein samples were irradiated in position L67 of the Ford reactor, University of Michigan (irradiation designated MN11), and received a total neutron fluence of approximately 10^{19} neutrons cm^{-2}. Hb3gr monitors were used to determine the irradiation parameters $J = 0.01785 \pm 0.00025$ and $\beta = 4.28 \pm 0.01$ (Kelley et al., 1986). Subsequently, β and J were used to calculate the fluence of fast and thermal neutrons, and thus to determine the abundance of Cl, Br, I and K measured as $^{38}Ar_{Cl}$, $^{80}Kr_{Br}$, $^{128}Xe_I$ and $^{39}Ar_K$ respectively. Calculated amounts of Br and I were corrected for production from resonant neutrons based on data from the Shallowater meteorite I-Xe standard. The resonant neutron flux was calculated as 2.8% of the total, accounting for approximately 25 and 45% of the neutron-produced $^{80}Kr_{Br}$ and $^{128}Xe_I$ respectively. The methods are described in detail by Johnson et al. (2000).

Approximately 80 mg of each sample was loaded into modified Nupro® valves and analysed by in vacuo crushing, five sequential crushes were obtained allowing the noble gas composition of the fluid to be determined. Subsequently 40 to 60 mg of the crushed residue was packed in aluminium foil and loaded into a tantalum resistance furnace. Samples were heated in steps of 30 min duration over a temperature range of 200°C to 1600°C at intervals of 200°C. Stepped heating extracts neutron-induced noble gas isotopes present in solid phases such as fluid inclusion daughter minerals (Kendrick et al., 2001). The halogen ratios Br/Cl and I/Cl are calculated from the total combined release of Cl, Br and I (measured as noble gas isotopes) during in vacuo crushing and stepped heating experiments (the complete data are tabulated in Appendix 1). A full discussion of the methods used is given in Kendrick et al. (2001).

In addition to data obtained from irradiated quartz, complimentary helium and argon isotope analyses (^3He, ^4He, ^{36}Ar and ^{40}Ar) have been obtained from unirradiated sulphide minerals (pyrite and chalcopyrite) present in the quartz veins of Silverbell, Globe-Miami, Pinto Valley and Ray. Helium and Ar measurements were obtained using a MAP 215 (Mass Analyser Products) mass spectrometer. Fluids were extracted from gram-sized samples using a hydraulically induced pressure of 12 tonnes. Helium and Ar were separated using a charcoal cold finger at liquid nitrogen temperature. Before isotopic analysis, noble gases were purified using two Zr-Al getters (SAES GP50 and NP10) to remove active gases. Detailed procedures are described in Stuart et al. (2000).

3. RESULTS AND DISCUSSION

The data are tabulated in Appendix 1; values representative of the included fluid composition are summarised in Table 2.

3.1. Halogens

Halogen ratios show a narrow range and are similar to values obtained from mantle samples defined by diamond and mid-ocean ridge basalts (MORB) (Fig. 2; Déruelle et al., 1992;

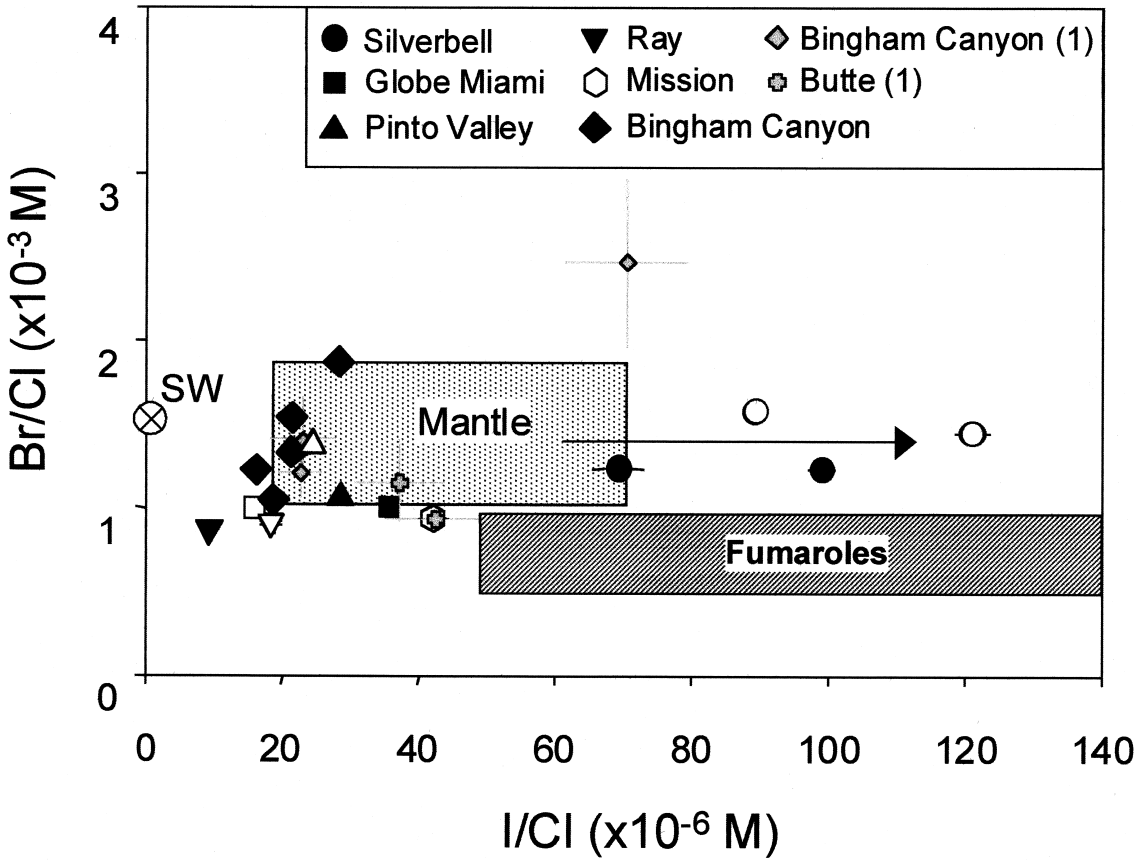

Fig. 2. Halogen composition of hydrothermal fluids included in porphyry copper quartz veins. The "mantle" box represents the range of halogen ratios measured in mantle diamond from Africa (Johnson et al., 2000) the "fumarole" box represents the halogen composition of volcanic fumaroles; see Bohlke and Irwin (1992a) for references. Previously determined halogen ratios for Bingham Canyon (Bingham Canyon-1) and Butte (Butte-1) are shown for reference (Irwin and Roedder, 1995). Solid symbols = potassic zone, open symbols = outer zones (Table 1). SW = seawater. Arrow indicates evolution of salinity away from the primary magmatic source.

Jambon et al., 1995; Johnson et al., 2000). PCD quartz have Br/Cl between 0.87 to 1.87 $\times 10^{-3}$ mole (M) and I/Cl between 9.34 to 42.2 $\times 10^{-6}$ M; these ratios are similar to those previously determined for Bingham Canyon and Butte (Irwin and Roedder, 1995) which are included in Figure 2 for comparison. Of the samples analysed in this study, only those from Silverbell have halogen compositions significantly different, with a higher I/Cl ratio of up to 121 $\times 10^{-6}$ M (Fig. 2).

The I/Cl ratios of all the samples are an order of magnitude greater than that of seawater (0.95 $\times 10^{-6}$ M). However, samples BC4 and SB6 have a Br/Cl ratio close to that of seawater (1.54 $\times 10^{-3}$ M) and with the exception of sample BC3, all the remaining samples have a significantly lower Br/Cl ratios. Schilling et al. (1978) estimated the Br/Cl ratio of the MORB source region to be close to that of seawater. However, from the halogen analysis of volcanic fumarole gases it has been argued that a magmatic fluid should have Br/Cl lower than the seawater value (Fuge, 1974; Sugiura et al., 1963). Bohlke and Irwin (1992a) compared the composition of fluids associated with the St. Austell granite and the average composition of volcanic fumaroles with Br/Cl in the range 0.5 to 1.0 $\times 10^{-3}$ M and I/Cl in the range 50 to 200 $\times 10^{-6}$ M, to characterise a magmatic brine. In a later study, Irwin and Roedder (1995) suggested that the low Br/Cl = 0.65 $\times 10^{-3}$ M and high I/Cl = 79 $\times 10^{-6}$ M values of the St. Austell fluid inclusions may reflect contamination of the magmatic brine with a minor crustal component. The St. Austell brine has been further constrained as 'magmatic' by Banks et al. (2000) using Cl isotopes, who also reported a Br/Cl ratio of 0.49 to 0.67 $\times 10^{-3}$ M. The lower limit of Br/Cl compositions measured in this study lies within the range of fumarole gas compositions supporting the magmatic origin, but with the exception of Silverbell, the I/Cl ratios are significantly lower.

The Br/Cl and I/Cl values measured in PCD do not preclude the involvement of sedimentary formation waters. However, the clustering of data points does indicate the operation of similar processes at five out of the six deposits studied and the range of compositions overlaps that observed in mantle samples (Fig. 2). Moreover, fluids associated with the crystallisation of an I-type granite may be expected to retain a magmatic/mantle signature. Therefore, it is considered that the halogen ratios are representative of a magmatic end-member.

With the exception of Silverbell, the compositional change between the outer zones and the inner potassic zone is small

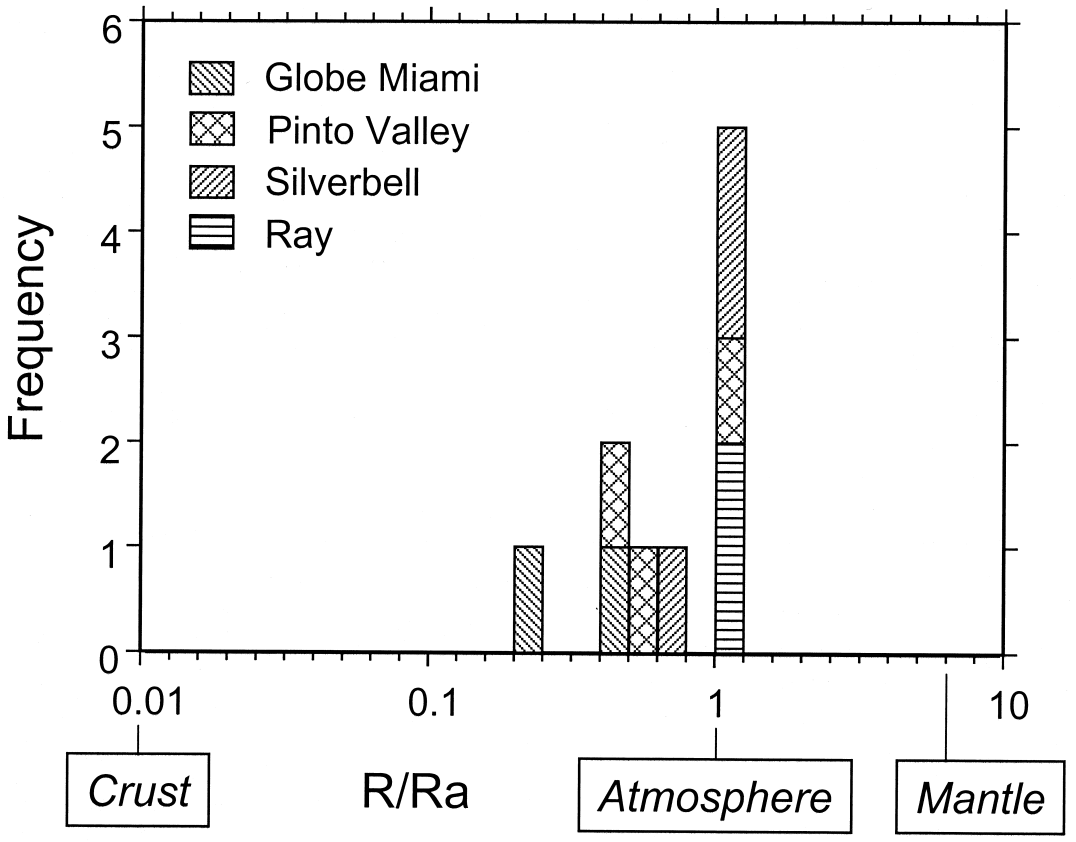

Fig. 3. Histogram of the $^{3}He/^{4}He$ composition of quartz vein hosted sulphide from Arizonan PCD, normalised to the atmospheric value (R/Ra = 1).

and both inner and outer zones have fluids with a mantle-like halogen signature. This is compatible with the potassic zone fluid having a magmatic origin and acquiring its salinity from a juvenile source. The preservation of this signature in the outer zones suggests magmatic fluids are present and that dilution or mixing can only have occurred with low salinity meteoric water.

The I/Cl value of fluids at Silverbell increases from the inner potassic to the outer propylitic zones and exceeds the range of values measured in mantle samples. Sedimentary formation waters can obtain elevated I/Cl ratios because I is enriched in sedimentary rocks as a result of sequestering by organic matter (Worden, 1996). The trend in I/Cl at Silverbell may indicate that formation waters have become entrained in the hydrothermal system of the outer propylitic zone, and to a lesser extent are also present in the potassic zone.

3.2. Helium

Helium data have been obtained from sulphide samples in the potassic and propylitic zones of Silverbell, Ray, Globe-Miami and Pinto Valley. Helium isotope ratios are between 0.3 and 1.7 Ra (Table 2; Fig. 3). The atmospheric He contribution can be determined from the $F^{4}He$ values, defined as the $^{4}He/^{36}Ar$ of a sample relative to the atmospheric $^{4}He/^{36}Ar$ value of 0.1655, such that a sample containing air will have an F value of 1. The $F^{4}He$ values for the sulphides are >1000 (Table 2). This means that ^{4}He is enriched by more than 1000 times above the atmospheric concentration and is more than 3000 times above the ^{4}He concentration in ASW ($F^{4}He = 0.18-0.28$). The high $F^{4}He$ values are evidence that the fluids contain negligible contributions of atmospheric He, and therefore the measured $^{3}He/^{4}He$ ratios result from mixing of crustal and mantle He sources. Unlike the $^{40}Ar/^{36}Ar$ ratios discussed later, the scarcity of helium in the atmosphere means the measured $^{3}He/^{4}He$ values do not reflect the extent of meteoric water involvement.

Post entrapment modification of the $^{3}He/^{4}He$ ratio is not considered to have been important. The low levels of neutron-induced ^{134}Xe from U released from quartz shows that the fluid inclusions contain low concentration of U and that production of ^{4}He since trapping has been negligible ($<0.01\%$).

Assuming binary mixing, the R/Ra ratio can be used to estimate the proportion of mantle (R_m) and crustal (R_c) components in the fluid. The proportion of mantle ^{4}He is calculated as:

$$\%\ \text{mantle He} = \frac{(R - R_c)}{(R_m - R_c)} \times 100$$

To use this expression, the composition of the two end-members must be defined. The crust typically has an R/Ra value in the range 0.01 to 0.05 (Tolstikhin, 1978), which is much lower than the MORB source region with an R/Ra of ~ 8. Using a value of 8 Ra as representative of pure mantle helium, and the

measured range in R/Ra of 0.3 to 1.72, gives the proportion of mantle helium as between 4 and 20%. However, magmatic bodies intruded into continental lithosphere usually have a lower $^3He/^4He$ than the MORB source due to the effects of crustal contamination and magmatic 'ageing'. Simmons et al. (1987) considered that a value of ~3 Ra may be more representative of evolved 'magmatic' bodies. Using the lower value of 3 Ra, it is estimated that the fluids contain between 10 and 58% of 'magmatic' He.

The relatively low R/Ra values of all the deposits in this study, indicate that crustal fluids are important in both the inner and outer zones of PCD. At Silverbell the R/Ra value decreases from 1.2 in the potassic zone to 0.84 in the propylitic zone (Table 2). The change is compatible with dilution of a magmatic fluid in the potassic zone, with formation water containing crustal He in the propylitic zone and is also in accord with the explanation given earlier for the outward increase in I/Cl values. In contrast, the R/Ra values at Ray, Pinto Valley and Globe-Miami increase outwards from values of 1.38, 0.76 and 0.32 to 0.60 in the potassic zones to higher values of 1.72, 1.15 and 0.69 in the outer zones, respectively (Table 2). This 'reverse' trend is based on a small number of samples, but suggests crustal fluids are important in the centre of these deposits and implies that fluids of different origin are thoroughly mixed throughout the hydrothermal system. The lowest measured R/Ra value of 0.3 indicates that > 90% of the ^4He in the potassic zone of Globe-Miami is of crustal origin.

3.3. Argon

3.3.1. Atmospheric Ar sources

$^{40}Ar/^{36}Ar$ and $Cl/^{36}Ar$ data obtained by in vacuo crushing (Fig. 4) have been corrected for in situ production of radiogenic ^{40}Ar since trapping. This was done using the published mineralisation ages (Table 1; Kendrick et al., 2001) and the K contents of the fluids measured as $^{39}Ar_K$. The correlations shown in Figure 4 represent binary mixing between two endmembers; a high salinity end-member with elevated $^{40}Ar/^{36}Ar$ and $Cl/^{36}Ar$, and a low salinity end-member with an atmospheric $^{40}Ar/^{36}Ar$ (296) and $Cl/^{36}Ar = 0$. The gradient of the mixing line is equivalent to the $^{40}Ar_E/Cl$ value of the high salinity component and is discussed in section 3.3.2.

The low salinity, low $^{40}Ar/^{36}Ar$ end-member may represent either, a mixture of air-saturated meteoric water (ASW) and palaeoatmospheric Ar included within the sample, or simply modern atmospheric Ar that has been adsorbed on to the sample as a contaminant. Although air contamination is almost impossible to eradicate entirely, the effects can be minimised by considering the analyses furthest from the atmospheric composition as being most representative of the high salinity end-member. Ideally the data should cluster around the maximum $^{40}Ar/^{36}Ar$ and $Cl/^{36}Ar$ values to be considered free of air contamination (Irwin and Roedder, 1995). The composition of the high salinity endmember estimated in this way for each sample are summarized in Table 2. The maximum $Cl/^{36}Ar$ measured in the samples can be used to estimate the ^{36}Ar concentration of the fluid (section 3.3.4). When the estimated ^{36}Ar concentrations in the fluid are combined with measured $^{84}Kr/^{36}Ar$ values, which are mainly in the range between air (0.02) and ASW (0.04), it appears that air contamination is significant in samples SB4, SB1, GM3, R3 and PV1.

3.3.2. $^{40}Ar_E/Cl$ and $Cl/^{36}Ar$ ratios

The highest $^{40}Ar_E/Cl$ value of 2.7×10^{-4} M is obtained from potassic zone fluids at Pinto Valley; this decreases to 1.4×10^{-4} M in the propylitic zone (Table 2). Such high $^{40}Ar_E/Cl$ are about 10 to 100 times higher than previously measured in crustal fluids (Turner and Bannon, 1992) and are similar to the range determined for fluids in diamonds and mantle xenoliths of 5 to 15×10^{-4} M (Johnson et al., 2000). The $^{40}Ar_E/Cl$ values measured at the other deposits are at least an order of magnitude lower (Table 2), being similar to values previously measured at Butte ~1 to 2.5×10^{-5} M (Irwin and Roedder, 1995), and implying the involvement of saline crustal fluids. Bingham Canyon and Mission have the lowest $^{40}Ar_E/Cl$ ratios of between 1.2×10^{-6} and 3.7×10^{-6} M (Fig. 4), these are within the range of values previously determined for Bingham Canyon at 0.5 to 8×10^{-6} M (Irwin and Roedder, 1995).

The Arizona PCD show a range in $Cl/^{36}Ar$ values of between 2.5 to 38.7×10^6 M this is identical to the range previously determined for granite-related mineral veins in southwest and northwest England ($2–40 \times 10^6$ M; Turner and Bannon, 1992). At Bingham Canyon the maximum $Cl/^{36}Ar$ ratio of potassic zone fluids (365×10^6 M; Fig. 4b) is an order of magnitude greater than that measured at any of the Arizonan deposits which are mostly $<40 \times 10^6$ M (Table 3, Fig. 4a). The $Cl/^{36}Ar$ value decreases to 5×10^6 M in the propylitic zone at Bingham Canyon, which is similar to the values in the propylitic zones of the Arizonan deposits (Table 2 and Fig. 4). The outward decrease in $Cl/^{36}Ar$ from the central potassic zone to the outer zones, at Pinto Valley, Ray and Bingham Canyon is compatible with fluids being diluted by meteoric water; as reflected by the outward decrease in salinity seen in all the deposits (Table 1). The high $Cl/^{36}Ar$ ratio measured in the potassic zone of Bingham Canyon (Fig. 4b) may be further explained by Ar loss during boiling of the hydrothermal fluid which would also account for the low $^{40}Ar_E/Cl$ value of this deposit. The greater extent of boiling at Bingham Canyon compared with the Arizonan deposits, gains some support from the relatively high abundance of high salinity and vapour inclusions observed in the Bingham samples (Table 1). The Bingham Canyon samples show a wide variation in $Cl/^{36}Ar$ and $^{40}Ar_E/Cl$ ratios of 66 to 365×10^6 M and 8.1 to 1.4×10^{-6} M respectively. Furthermore, the potassic samples BC5-A, B and C, show significant variation in these ratios across a single vein reflecting the differing extent to which boiling has affected fluids from within the same zone on a local scale. The samples with the highest $^{40}Ar_E/Cl$ ratio are dominated by the vapour phase inclusions, while samples having lower $^{40}Ar_E/Cl$ ratios may contain a higher proportion of the liquid residue.

The $Cl/^{36}Ar$ and $^{40}Ar_E/Cl$ are influenced by the concentration of Ar and salinity of the fluid, however these ratios do not appear to be related in a systematic manner in the other deposits. The reason for this is probably that the source of $^{40}Ar_E$ and Cl, most likely K-rich crustal rocks or the upper mantle, is unrelated to the source of ^{36}Ar, which is from the atmosphere possibly by way of meteoric water.

3.3.3. Crust and mantle $^{40}Ar_E$ and ^4He sources

The measured $^{40}Ar/^{36}Ar$ composition of PCD fluids range from 317 in the propylitic alteration at Bingham Canyon to 3211 in the potassic zone of Pinto Valley (Table 2). Irwin and

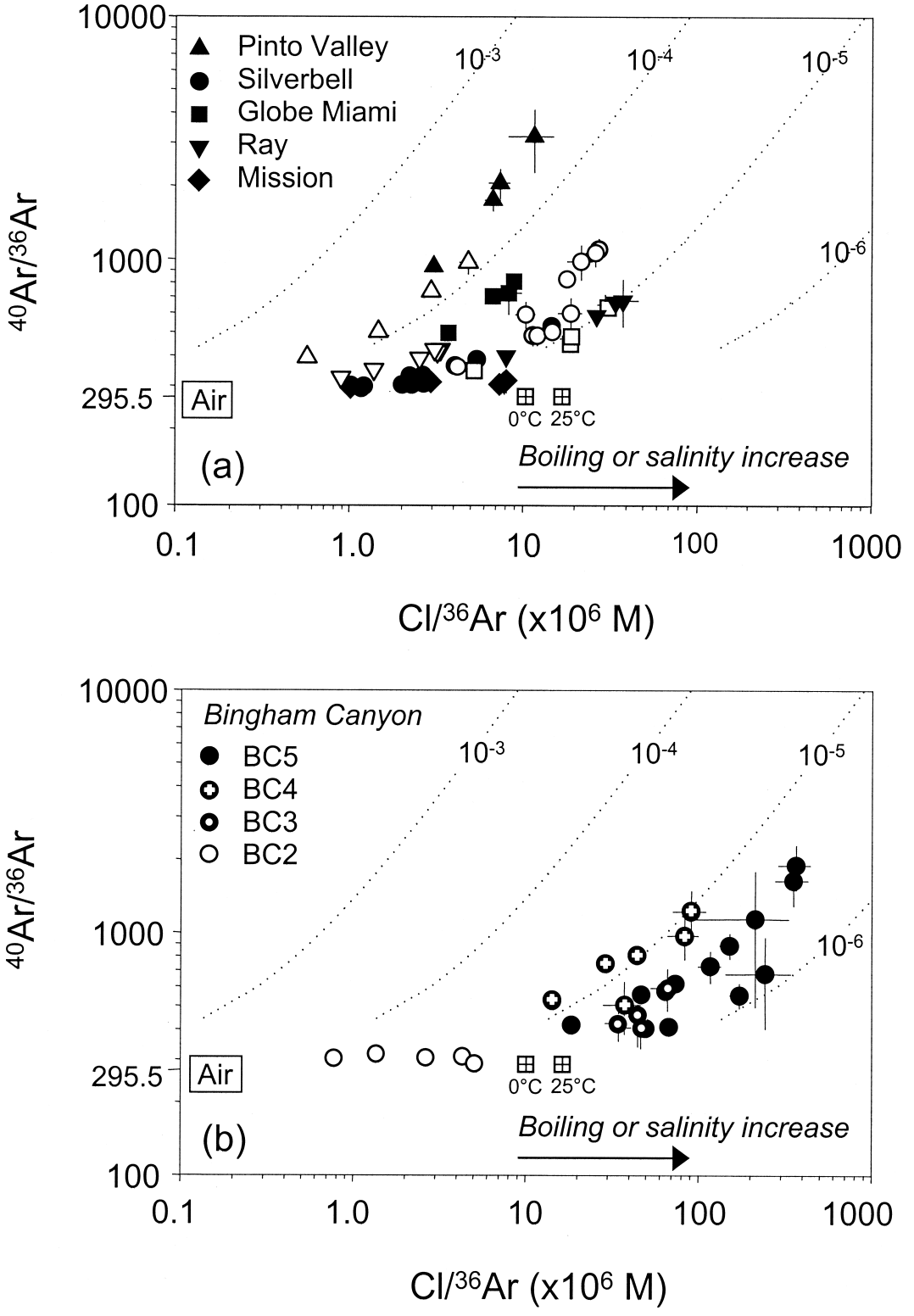

Fig. 4. Log-log plots of $^{40}Ar/^{36}Ar$ against $Cl/^{36}Ar$ for (a) Arizonan PCD, and (b) Bingham Canyon, Utah. Trajectories of $^{40}Ar_E/Cl$ with an intercept of 296 are plotted as dotted lines and appear as curves. Data are on binary mixing arrays (parallel to the trajectories) between a high salinity end-member with an elevated $^{40}Ar/^{36}Ar$ value, probably an intimate mix of mantle and crustal fluids, and a low salinity end-member with an atmospheric $^{40}Ar/^{36}Ar$ ratio, consistent with meteoric water and air. For each sample, the point with the highest $^{40}Ar/^{36}Ar$ and $Cl/^{36}Ar$ ratio is considered most free of air contamination and has been tabulated in Table 2. Data from potassic zone samples shown by solid symbols, outer zone samples by open symbols.

Table 3. $^{40}Ar/^{36}Ar$ composition of quartz and sulphide fluid inclusions

	Silverbell		Globe-Miami		Pinto Valley		Ray		Mission	Bingham Canyon
	Q[a]	S	Q	S	Q	S	Q	S	Q	Q
Potassic										
$^{40}Ar/^{36}Ar$	372	914	824	907	3211	1063	677	547		1222
% $^{40}Ar_E$	21	68	64	67	91	72	56	46		76
Outer zone										
$^{40}Ar/^{36}Ar$	1112	924	662	612	985	603	433	813	323	317
% $^{40}Ar_E$	73	68	55	52	70	51	32	64	9	7

[a] Q and S distinguish quartz and sulphide fluid inclusion compositions.

Roedder (1995) reported a $^{40}Ar/^{36}Ar$ value of 3700 at Bingham Canyon, and 650 at Butte that cover the same range measured in the present study. $^{40}Ar/^{36}Ar$ values higher than the atmospheric ratio indicates the presence of a significant proportion of $^{40}Ar_E$ of mantle or crustal origin. The proportion of $^{40}Ar_E$ can be estimated using the maximum measured $^{40}Ar/^{36}Ar$ value $[(^{40}Ar/^{36}Ar)_{max}]$ as follows:

$$\%\ ^{40}Ar_E = \frac{(^{40}Ar/^{36}\ Ar)_{max} - 296}{(^{40}Ar/^{36}/\ Ar)_{max}} \times 100$$

Estimates of the $^{40}Ar_E$ contents for the inner potassic and outer zones are given in Table 3. The $^{40}Ar_E$ of 20% for the potassic zone at Silverbell is probably an underestimate due to the effects of air contamination, a more realistic approximation, based on the $^{40}Ar/^{36}Ar$ in sulphide, is 67% $^{40}Ar_E$ (Table 3). Both the $^{40}Ar/^{36}Ar$ value and the proportion of $^{40}Ar_E$ decrease from the central potassic zone to the outer zones in all the deposits except Silverbell (Table 3); this is consistent with the dilution of fluids containing $^{40}Ar_E$ by meteoric water. The slight outward increase in $^{40}Ar/^{36}Ar$ at Silverbell can be attributed to the involvement of formation waters containing crustal $^{40}Ar_E$ in the propylitic zone of that deposit.

The $^{40}Ar/^{36}Ar$ of fluid inclusions in sulphide tend to show slightly less variation than in quartz fluid inclusions. $^{40}Ar/^{36}Ar$ values are between 547 and 1063 in sulphide compared to 323 to 3211 in quartz (Table 3). The variation in the sulphide $^{40}Ar/^{36}Ar$ values corresponds to between 46 and 72% $^{40}Ar_E$. The $^{40}Ar_E$ content of the fluid from which the quartz gangue formed appears to be more variable than fluid responsible for precipitation of the ore minerals. The meteoric water reduces the $^{40}Ar/^{36}Ar$ ratio in the outer zone, but has little effect on the R/Ra ratio.

The range in $^{40}Ar_E/^4He$ values of between 0.37 (GM3) and 1.8 (R3) are, with the exception of the lowest value (GM3), above the crustal and mantle $^{40}Ar_E/^4He$ production ratios of 0.2 and 0.5 respectively (Fig. 5). The $^{40}Ar_E/^4He$ ratio and the $^3He/^4He$ ratio do not exhibit a well defined correlation, suggesting that two independent processes account for the variation in $^{40}Ar_E/^4He$ and $^3He/^4He$. The variation in $^3He/^4He$ ratio results from mixing different quantities of crustal and mantle-derived volatile components. The high $^{40}Ar_E/^4He$ ratios can be explained by either loss of He due to its relatively high volatility, or enrichment in $^{40}Ar_E$, derived from crust already degassed of He. However, the latter process would be expected to lead to a correlation between $^{40}Ar_E/^4He$ and $^{40}Ar/^{36}Ar$ (Table 2) which is not observed, thus making He loss the favoured explanation for the variation in $^{40}Ar_E/^4He$ values.

3.3.4. ^{36}Ar concentration

The concentration of ^{36}Ar can be estimated by combining the $Cl/^{36}Ar$ value with salinity measurements based on thermometric analysis (Turner and Bannon, 1992). The main limitation to this approach is in the accuracy with which the bulk salinity of fluid inclusion populations can be obtained. Estimates of the average fluid inclusion salinity have been made based on thermometric analyses of individual fluid inclusion types and a qualitative assessment of their occurrence (Table 1). Despite the limitations imposed by averaging fluid inclusions of different type and salinity, we believe that some useful inferences can be made from the derived ^{36}Ar concentrations.

The estimated concentrations of ^{36}Ar in the inner and outer zones of the PCD are given in Table 4. The ^{36}Ar concentration for potassic fluids at Bingham Canyon (BC5) are low at 0.2 to 0.6×10^{-6} cm^3 STP/g H_2O (calculated assuming a $Cl/^{36}Ar$ of $117–365 \times 10^6$ and an average salinity of 17 wt. % NaCl equ.; see Tables 1 and 2). This is below the ^{36}Ar-concentration of ASW (0.96×10^{-6} cm^3 STP/g at 25°C and 1.68×10^{-6} cm^3 STP/g at 0°C; references in Ozima and Podosek, 1983). Irwin and Roedder (1995) estimated a similarly low ^{36}Ar-concentra-

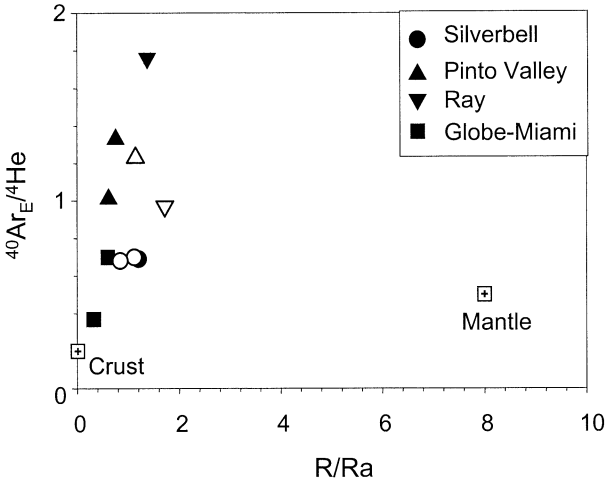

Fig. 5. $^3He/^4He$ versus $^{40}Ar_E/^4He$ for Arizonan PCD. $^{40}Ar_E/^4He$ values in PCD fluids are higher than the crustal and MORB mantle production ratios. Solid symbols = potassic zone, open symbols = outer zones.

Table 4. Estimated ^{36}Ar concentrations in fluids ($\times 10^{-6}$ cm^3 STP/g H_2O) of PCD deposits

Zone	Silverbell		Globe-Miami		Pinto Valley		Ray		Mission		Bingham Canyon	
Potassic	SB4	7.8	GM4	4.3	PV6	4.0	R1	6.0			BC5	0.2
Outer zone	SB6	1.1	GM3	0.5	PV1	4.0	R3	6.0	M3	1.9	BC2	1.6

tion of 0.1 to 0.3 $\times 10^{-6}$ cm^3 STP/g for Bingham Canyon which they used as evidence that the fluids had a magmatic origin. However, the low ^{36}Ar concentration is also compatible with Ar loss during boiling of hydrothermal fluids. Based on an average salinity of 2 wt % NaCl, the propylitic zone at Bingham Canyon has a ^{36}Ar-concentration of 1.56 $\times 10^{-6}$ cm^3 STP/g, this is within the range of values for ASW indicating that this zone is dominated by meteoric water. Irwin and Roedder (1995) reported a similar value of 2.17 $\times 10^{-6}$ cm^3 STP/g for meteoric fluids included in quartz at the Butte PCD.

In contrast to Bingham Canyon, the ^{36}Ar concentrations of fluids at the Arizonan deposits are equal to or above that of ASW (Table 4). This indicates a significant involvement of externally derived surface fluid (meteoric or formation water) in both the potassic and propylitic zones of these deposits, and is consistent with the lack of evidence for boiling amongst the fluid inclusion populations of these samples (Table 1).

The high ^{36}Ar concentration of $\geq 4.0 \times 10^{-6}$ cm^3 STP/g H_2O in the potassic samples from Silverbell (SB4) and Globe-Miami (GM3), and the outer zone samples from Ray (R3) and Pinto Valley (PV1) are most easily explained as a result of air contamination (Table 4). These samples have $^{84}Kr/^{36}Ar$ values (Table 2) that are between the atmospheric ratio (0.02) and 0.03, well below the ASW value (0.04) and supporting significant air contamination (>50%). The potassic zone sample from Pinto Valley (PV6) also has a high ^{36}Ar concentration but this is combined with a $^{84}Kr/^{36}Ar$ value of ASW (Table 2) thus, unless the $^{84}Kr/^{36}Ar$ was initially above that of ASW, air contamination does not provide a good explanation for the source of ^{36}Ar in this sample. One possibility is that ^{36}Ar may have been acquired through interaction with fine-grained sediment which can be enriched in adsorbed atmospheric noble gases (see Ozima and Podosek, 1983).

3.5. Elemental Fractionation of Ar, Kr and Xe by Boiling

The $^{84}Kr/^{36}Ar$ and $^{40}Ar/^{36}Ar$ ratios of fluids from Bingham Canyon and Pinto Valley show a marked decrease between the potassic and propylitic zones (Fig. 6a) which is compatible with an influx of meteoric water. Additionally, the high $^{84}Kr/^{36}Ar$ values of the Bingham Canyon potassic zone samples, BC5-A (0.264) and BC4 (0.058), which are above the ASW value (0.04) suggests significant Kr/Ar fractionation has occurred. This is most easily explained by preferential loss of more volatile Ar during boiling.

Previously, Irwin and Roedder (1995) measured $^{84}Kr/^{36}Ar$ values up to twice the ASW value at Bingham Canyon (≤ 0.086) which they interpreted as being characteristic of a magmatic fluid. However, the low ^{36}Ar-concentration, and the elevated $Cl/^{36}Ar$ and $^{84}Kr/^{36}Ar$ ratios observed in sample BC5-A (Tables 2 and 4), are all characteristics that can be best explained by Ar loss during boiling. This finding is supported by the FXe values determined for sample BC5-A, which correlates with FKr (Fx = $(X/^{36}Ar)$sample/$(X/^{36}Ar)$air where $(^{129}Xe/^{36}Ar)$air = 0.7237 $\times 10^{-3}$ and $(^{84}Kr/^{36}Ar)$air = 0.0207; Fig. 6b) indicating that the hydrothermal fluid has preferentially lost noble gases corresponding to their volatility, Ar>Kr>Xe. Similar fractionations have been attributed to partitioning of noble gases between liquid and steam in the geothermal waters of Yellowstone national park, U.S., although in this system the fractionation factors are somewhat lower FKr <4 and FXe<16 (Kennedy et al., 1985). To attain the extreme values of FKr≥10 and FXe≥100 may require a multistage fractionation process.

The $^{84}Kr/^{36}Ar$ values of samples BC5-B (0.038) and BC5-C (0.044) from the same vein and situated adjacent to sample BC5-A, are significantly lower. In contrast to BC5-A these samples have F values within or close to the range explained by mixing of air and ASW. This may be because boiling has been less important in these fluids, or that samples BC5-B and BC5-C contain fluid inclusions dominated by the vapour phase of boiling compared to sample BC5-A which contains a higher proportion of liquid residue. Although noble gas ratios Kr/Ar and Xe/Ar are correlated within samples BC5-A, B and C; the highest Kr/Ar ratio does not correlate with the highest $Cl/^{36}Ar$, lowest $^{40}Ar_E/Cl$ ratio and lowest ^{36}Ar concentration (Tables 2 and 4) as may have been expected if boiling was the only process involved. This inconsistency may be attributed to either variations in salinity, which affect the calculated ^{36}Ar concentration, small but variable extents of air contamination, or the differing sources of $^{40}Ar_E$, ^{84}Kr, ^{36}Ar, and Cl.

The lack of a systematic difference in $^{84}Kr/^{36}Ar$ between the potassic and propylitic zones of the other deposits (Table 2) is probably related to the variable extent of air contamination. However at Silverbell, it is also possible that the higher $^{84}Kr/^{36}Ar$ of the propylitic zones may result from an influx of sedimentary formation water with a higher ^{84}Kr concentration.

4. SUMMARY AND CONCLUSIONS

Combined noble gas and halogen analysis provides important new insight as to the source and interactions of mineralising fluids in PCD. The findings are consistent with interpretations based on existing fluid inclusion and stable isotope data, but unlike O and H isotopes, understanding of the noble gases and halogens is largely unaffected by processes involving isotopic equilibration and exchange with host rocks.

The data acquired in this study shows considerable variation, not all of the PCD characteristics are displayed by a single sample, or by a single deposit. However, taken together the samples provide a comprehensive overview of the features most typical of PCD mineralisation, including the effects of

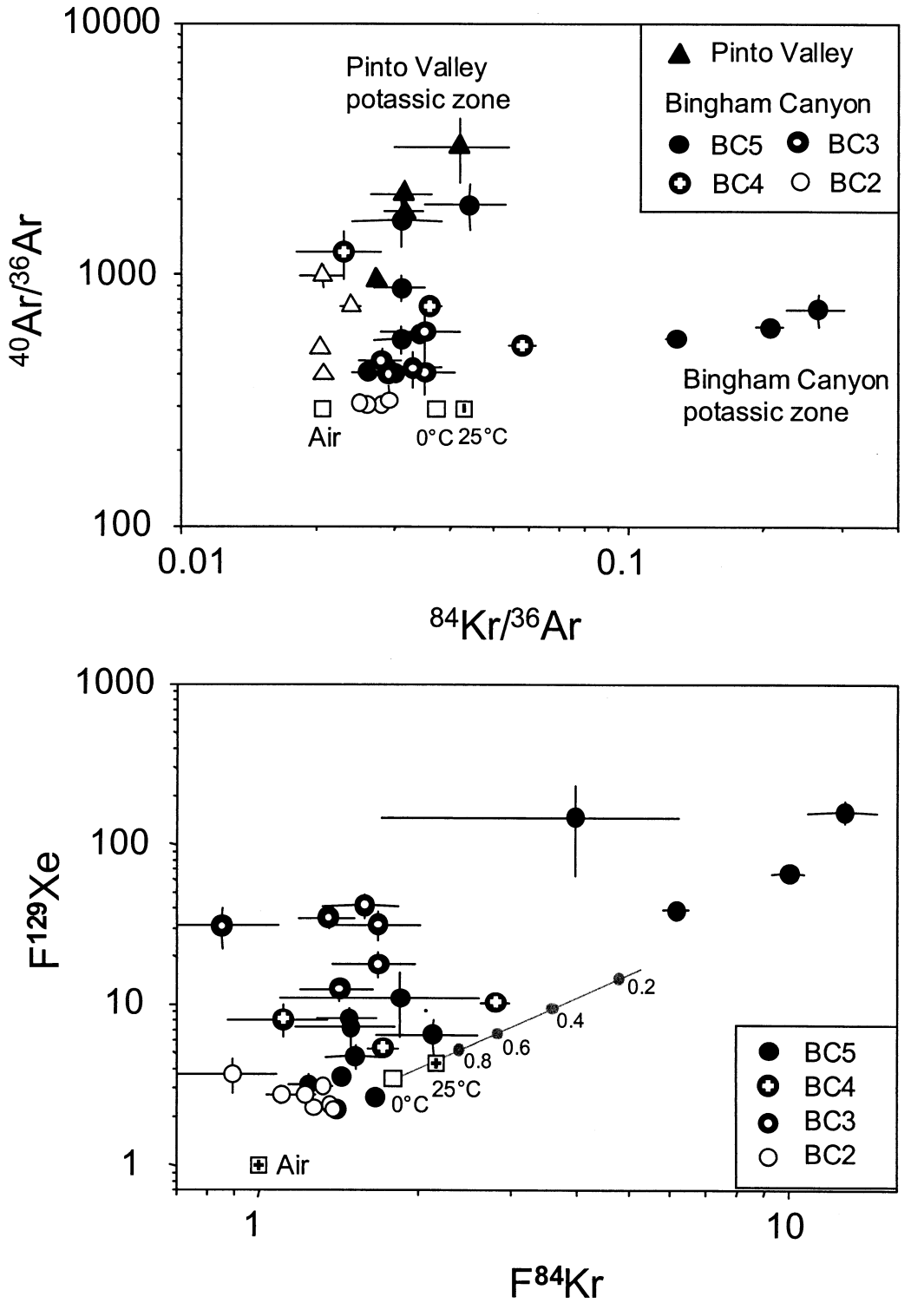

Fig. 6. (a) $^{84}Kr/^{36}Ar$ versus $^{40}Ar/^{36}Ar$ for Pinto Valley and Bingham Canyon. The data are compatible with mixing of two fluid end-members; a high salinity end-member dominates the potassic zone having a high $^{40}Ar/^{36}Ar$ value and $^{84}Kr/^{36}Ar$ value above that of ASW, at Bingham Canyon this attributed to the boiling. The other endmember fluid, dominant in the propylitic zone, has an atmospheric $^{40}Ar/^{36}Ar$ ratio compatible with meteoric water. $^{84}Kr/^{36}Ar$ are between the ASW (shown for 0° and 25°C) and air values suggesting air contamination of the samples. (b) An F-plot showing the effects of boiling at Bingham Canyon. FKr and FXe values exceed the ASW values: $FX = (X/^{36}Ar)_{sample}/(X/^{36}Ar)_{air,}$ where $^{129}Xe/^{36}Ar_{air}=0.7237 \times 10^{-3}$ and $^{84}Kr/^{36}Ar_{air}=0.0207$. The curve for Rayleigh distillation is calculated for open-system boiling at 100°C assuming an initial noble gas composition of air saturated water at 0°C. In both (a) and (b) square symbols mark the compositions of ASW (at 0° and 25°C) and air.

boiling and the characteristics of a high salinity potassic fluid, which are best seen in the potassic samples from Bingham Canyon. The main findings of this work are summarised as follows:

1. Correlation of $^{40}Ar/^{36}Ar$ with $Cl/^{36}Ar$ indicates that fluids at all deposits result from mixing of high and low salinity end-members. Low $^{84}Kr/^{36}Ar$ values between air (0.02) and ASW (0.04), and $^{40}Ar/^{36}Ar$ ratios close to 296, indicate the low salinity end-member is a mixture of meteoric water and air. The high salinity end-member has an elevated $^{40}Ar/^{36}Ar$ ratio, shows a constant $^{40}Ar_E/Cl$ in the range 1.1×10^{-6} to 1.4×10^{-4} M, and is interpreted as a mixture of $^{40}Ar_E$ from mantle and crustal sources.
2. Br/Cl and I/Cl have a relatively narrow range of values at each of the deposits except Silverbell ($I/Cl = 9.3–42.2 \times 10^{-6}$ M; $Br/Cl = 0.9–1.9 \times 10^{-3}$ M); these overlap with the range determined in mantle fluids suggesting salinity was acquired primarily from a juvenile source.
3. $^{3}He/^{4}He$ ratios provide unambiguous evidence for mantle derived magmatic volatiles. However, values in the range 0.3 to 1.7 Ra indicate that crustal fluids are more important than previously realised. In the Arizonan deposits studied it is estimated that between 40 and 90% of the He has a crustal origin.
4. The potassic zone fluids contain a mixture of magmatic, crustal and meteoric-derived noble gases. The contribution of Ar from meteoric water in the potassic zone of each deposit has been estimated from the maximum $^{40}Ar/^{36}Ar$ value measured in quartz at that deposit. Values range between approximately 10% at Pinto Valley and 40% at Ray. The amount of mantle He contributed to the potassic zone fluids, based on the $^{3}He/^{4}He$ ratio of sulphide samples, is between a minimum of 4% at Globe-Miami and a maximum of 17% at Ray.
5. Fluids from the outer zone also contain noble gases from magmatic, crustal and meteoric sources. He isotope data indicate that at some deposits (Ray, Globe-Miami and Pinto Valley), crustal volatiles are slightly more dominant in the potassic zones than they are in the outer zones.
6. Silverbell shows the clearest evidence for the involvement of sedimentary formation waters; this is apparent from the increase in I/Cl value in the outer zone.
7. Analysis of some adjacent samples from a single vein in the potassic zone of Bingham Canyon show low concentrations of ^{36}Ar (below that of ASW), high $Cl/^{36}Ar$, low $^{40}Ar_E/Cl$, and highly fractionated $^{84}Kr/^{36}Ar$, $^{129}Xe/^{36}Ar$ ratios. This is interpreted as evidence for boiling of the fluid and is supported by samples having a high proportion of vapour-dominated inclusions. There is variability between samples from the vein indicating that different parts of the vein are dominated by the liquid and vapour phase of boiling and therefore that fluid flow may have been pulsed.

Acknowledgments—We wish to express our thanks to D. Blagburn and B. Clementson for technical support in the noble gas laboratory, P. Harrop for assistance with helium analyses and C. Thrower for help with sample preparation. J. Ford's contribution to the project is acknowledged and the authors are very grateful to Sal Anzalone (ASARCO), R. Cummings, E. John, D. Laux, G. Lenzie, C. Philip for facilitating and assistance with sample collection. Access to mines was provided by ASARCO and Rio Tinto (Bingham Canyon). We thank E. Roedder, D.L. Pinti and an anonymous reviewer for their helpful comments which have improved the manuscript. Funding was provided by a NERC studentship (MK) and a Royal Society university research fellowship (RB).

Associate editor: J. Matsuda

REFERENCES

Banks D. A., Green R., Cliff R. A. and Yardley B. W. D. (2000). Chlorine isotopes in fluid inclusions: determination of the origins of salinity in magmatic fluids. *Geochim. Cosmochim. Acta* **64,** 1785–1789.

Banks N. G., Cornwall H. R., Silberman M. L., Creasey S. C. and Marvin R. F. (1972) Chronology of intrusion and ore deposition at Ray, Arizona: Part I, K-Ar Ages. *Econ. Geol.* **67,** 864–878.

Beane R. T. J. and Titley S. R. (1981) Porphyry copper deposits, alteration and mineralisation, part II. *Econ. Geol.* **75th anniversary volume,** 235–269.

Bohlke J. K. and Irwin J. J. (1992a) Laser microprobe analyses of Cl, Br, I, and K in fluid inclusions: implications for the sources of salinity in some ancient hydrothermal fluids. *Geochim. Cosmochim. Acta* **56,** 203–225.

Bohlke J. K. and Irwin J. J. (1992b) Laser microprobe analyses of noble gas isotopes and halogens in fluid inclusions: analyses of microstandards and synthetic inclusions in quartz. *Geochim. Cosmochim. Acta* **56,** 187–201.

Bohlke J. K. and Irwin J. J. (1992c) Brine history indicated by argon, krypton, chlorine, bromine, and iodine analyses of fluid inclusions from the Mississippi Valley type lead-fluorite-barite deposits at Hansonburg, New Mexico. *Earth Planet. Sci. Lett.* **110,** 51–66.

Bowman J. R., Parry W. T., Kropp W. P. and Kruer S. A. (1987) Chemical and isotopic evolution of hydrothermal solutions at Bingham, Utah. *Econ. Geol.* **82,** 395–428.

Burgess R. and Parsons I. (1994) Argon and halogen geochemistry of hydrothermal fluids in the Loch Ainort granite, Isle of Skye, Scotland. *Contrib. Mineral. Petrol.* **115,** 345–355.

Burnard P., Graham D. and Turner G. (1997) Vesicle-specific noble gas analyses of "popping rock"; implications for primordial noble gases in the Earth. *Science* **276,** 568–571.

Creasey S. C. (1980) Chronology of intrusion and deposition of porphyry copper ores, Globe-Miami district, Arizona. *Econ. Geol.* **75,** 830–844.

Crocetti C. A. and Holland H. D. (1989) Sulfur-lead isotope systematics and the composition of fluid inclusions in galena from the Viburnum Trend, Missouri. *Econ. Geol.* **84,** 2196–2216.

Déruelle B., Dreibus G and Jambon A. (1992) Iodine abundances in oceanic basalts: implications for Earth dynamics. *Earth Planet. Sci. Lett.* **108,** 217–227.

Dilles J. H., Soloman G. C., Taylor H. P. Jr. and Einaudi M. (1992) Oxygen and hydrogen isotope characteristics of hydrothermal alteration at the Ann-Mason porphyry copper deposit, Yerington, Nevada. *Econ. Geol.* **87,** 44–63.

Eastoe C. J. (1978) A fluid inclusion study of the Panguna porphyry copper deposit, Bougainville, Papua New Guinea. *Econ. Geol.* **73(5),** 721–748.

Fuge R. (1974) Bromine, iodine. In *Handbook of Geochemistry* (ed. K. H. Wedepohl), pp. Chap. 35 and 53. Springer-Verlag.

Guilbert J. M. and Lowell J. D. (1974) Variations in zoning patterns in porphyry ore deposits. *Can. Min. Metallurg. Bull.* **742,** 99–109.

Irwin J. J. and Reynolds J. H. (1995) Multiple stages of fluid trapping in the Stripa granite indicated by laser microprobe analysis of Cl, Br, I, K, U, and nucleogenic plus radiogenic Ar, Kr, and Xe in fluid inclusions. *Geochim. Cosmochim. Acta* **59,** 355–369.

Irwin J. J. and Roedder E. (1995) Diverse origins of fluid inclusions at Bingham (Utah, USA), Butte (Montana, USA), St. Austell (Cornwall, UK) and Ascension Island (mid-Atlantic, UK), indicated by laser microprobe analysis of Cl, K, Br, I, Ba + Te, U, Ar, Kr, and Xe. *Geochim. Cosmochim. Acta* **59,** 295–312.

Jambon A., Déruelle B., Dreibus G. and Pineau F. (1995) Chlorine and bromine abundance in MORB: the contrasting behaviour of the

Mid-Atlantic Ridge and East Pacific Rise and implications for the chlorine geodynamic cycle. *Chem. Geol.* **126,** 101–117.

Johnson L. H., Burgess R., Turner G., Milledge J. H., and Harris J. W. (2000). Noble gas and halogen geochemistry of mantle fluids: comparison of African and Canadian diamonds. *Geochim. Cosmochim. Acta* **64,** 717–732.

Kelley S., Turner G., Butterfield A. W., and Shepherd T. J. (1986) The source and significance of argon isotopes in fluid inclusions from areas of mineralization. *Earth Planet. Sci. Lett.* **79,** 303–318.

Kendrick M., Burgess R., Pattrick R. A. D. and Turner G. (2001) Halogen and Ar-Ar age determinations of fluid inclusions in quartz veins from porphyry copper deposits using complementary noble gas extraction techniques. *Chem. Geol.* **177,** 351–370.

Kennedy B. M., Lynch M. A., Reynolds J. H. and Smith S. P. (1985) Intensive sampling of noble gases in fluids at Yellowstone: I. Early overview of the data; regional patterns. *Geochim. Cosmochim. Acta.* **49,** 1251–1261.

Lanier G., John E. C., Swensen A. J., Reid J., Bard C. E., Caddey S. W. and Wilson J. C. (1978) General geology of the Bingham Mine, Bingham Canyon, Utah. *Econ. Geol.* **73,** 1228–1241.

Livingston D. E. (1973) A Plate tectonic hypothesis for the genesis of porphyry copper deposits of the southern Basin and Range Province. *Earth Planet. Sci. Lett.* **20,** 171–179.

Moore W. J. and Nash J. T. (1974) Alteration and fluid inclusion studies of the porphyry copper ore body at Bingham, Utah. *Econ. Geol.* **69,** 631–645.

Nash J. T. (1976) Fluid inclusion petrology, data from porphyry copper deposits and applications to exploration. *U.S.G.S. Prof. Paper* **907-D,** 16.

O'Nions R. K. and Oxburgh E. R. (1988) Helium, volatile fluxes and the development of continental crust. *Earth Planet. Sci. Lett.* **90,** 331–347.

Ozima M. and Podosek F. A. (1983) Noble gas geochemistry. Cambidge University Press, Cambridge.

Phillips C. H., Gambell N. A., and Fountain D. S. (1974) Hydrothermal alteration, mineralisation and zoning in the Ray Deposit. *Econ. Geol.* **69,** 1237–1250.

Richard K. and Courtright J. H. (1966) Structure and Mineralisation at Silverbell, Arizona. In *Geology of the Porphyry copper Deposits, Southwestern North America* (ed. S. R. Titley, and C.J. Hicks). University of Arizona Press.

Roedder E. (1971) Fluid inclusion studies on the porphyry-type ore deposits at Bingham, Utah, Butte, Montana, and Climax, Colorado. *Econ. Geol.* **66,** 98–120.

Roedder E. (1984) Fluid Inclusions. Min. Soc. America. *Rev. Mineral.* **12,** 644.

Schilling J. C., Unni C. K., and Bender M. L. (1978) Origin of chlorine and bromine in the oceans. *Nature.* **273,** 631–636.

Sheppard S. M. F., Nielson R. L., and Taylor H. P. Jr. (1969) Oxygen and hydrogen isotope ratios of clay minerals from porphyry copper deposits. *Econ. Geol.* **64,** 755–777.

Sheppard S. M. F. and Gustafson L. (1976) Oxygen and hydrogen isotopes in the porphyry copper deposit at El Salvador, Chile. *Econ. Geol.* **71,** 1549–1559.

Sheppard S. M. F., Nielson R. L., and Taylor H. P. Jr. (1971) Hydrogen and oxygen isotope ratios in minerals from porphyry copper deposits. *Econ. Geol.* **66,** 515–542.

Sheppard S. M. F. and Taylor H. P. J. (1974) Hydrogen and oxygen isotope evidence for the origin of water in the Boulder batholith and Butte ore deposits, Montana. *Econ. Geol.* **69,** 926–946.

Simmons S. F., Sawkins F. J. and Schlutter D. J. (1987) Mantle derived helium in two Peruvian hydrothermal ore deposits. *Nature.* **329,** 429–432.

Smith S. P. and Kennedy B. M. (1983) The solubility of noble gases in water and in NaCl brine. *Geochim. Cosmochim. Acta* **47,** 503–515.

Stuart F. M., Allam R. M., Harrop P. J., Fitton J. G. and Bell B. R. (2000). Constraints on mantle plumes from the helium isotopic composition of basalts from the Br. Tertiary Igneous Province. *Earth Planet. Sci. Lett.* **177,** 273–285.

Sugiura T., Mizutani Y. and Oana S. (1963) Fluorine, chlorine, bromine, and iodine in volcanic gases. *J. Earth Sci. (Nagoya University)* **11,** 272–278.

Taylor H. P. (1997) Oxygen and hydrogen isotope relationships in hydrothermal mineral deposits. In *Geochemistry of hydrothermal ore deposits* (ed. H. L. Barnes), pp. 229–302. John Wiley and Sons, Inc.

Titley S. R. (1982) The style and progress of mineralisation and alteration in porphyry copper systems, American southwest. In *Advances in geology of the porphyry copper deposits, Southwestern North America* (ed. S. R. Titley), pp. 93–116. University of Arizona Press.

Titley S. R. (1994) Evolutionary habits of hydrothermal and supergene alteration in intrusion-centred ore systems: Southwestern North America. In *Alteration and alteration processes associated with ore-forming systems* (ed. D. R. Lentz) Vol. 11, pp. 237–260. Geological Association of Canada, short course notes.

Titley S. R. (1995) Geological summary and perspective of porphyry copper deposits in Southwestern North America. In *Porphyry Copper Deposits of the American Cordillera* (ed. F. W. Pierce and J. G. Bolm)Vol. 20, pp. 6–20. Arizona Geological Society Digest.

Titley S. R., Anzalone S. A. and Anthony E. Y. (1989) Porphyry copper deposits in the American southwest, Tucson to Globe-Miami, Arizona July 19–23 1989. Field trip guidebook T338, Tucson to Globe-Miami, Ariz., July 19–23, 1989, AGU Washington

Tolstikhin I. N. (1978) A review: some recent advances in isotope geochemistry of light rare gases. In *Terrestrial rare gases*, (eds. E. C. Alexander and M. Ozima), pp. 27–62. Japan Scientific Society Press, Tokyo.

Turner G. and Bannon M. P. (1992) Argon isotope geochemistry of inclusion fluids from granite-associated mineral veins in southwest and northeast England. *Geochim. Cosmochim. Acta* **56,** 227–243.

Turner G., Burnard P., Ford J. L., Gilmour J. D., Lyon I. C. and Stuart F. M. (1993) Tracing fluid sources and interactions. *Phil. Trans. Roy. Soc. Lond. A.* **344,** 127–140.

Viets J. G., Hofstra A. H. and Emsbo P. (1996) Solute compositions of fluid inclusions in sphalerite from North American and European Mississippi Valley-Type ore deposits: ore fluids derived from evaporated seawater. *Soc. Econ. Geol. Spec. Pub.* **4,** 465–482.

Warnaars F. W., Smith W. H., Bray R. E., Lanier G. and Shafiqullah M. (1978) Geochronology of igneous intrusions and porphyry copper mineralisation at Bingham, Utah. *Econ. Geol.* **73,** 1242–1249.

Worden R. H. (1996) Controls on halogen concentrations in sedimentary formation waters. *Min. Mag.* **60,** 259–274.

APPENDIX 1

Sample	Cl mol ($\times 10^{-9}$)	Br mol ($\times 10^{-12}$)	I mol ($\times 10^{-15}$)	^{40}Ar mol ($\times 10^{-15}$	^{36}Ar mol ($\times 10^{-15}$)	^{84}Kr mol ($\times 10^{-18}$)	^{129}Xe mol ($\times 10^{-18}$)
BC5-A							
Crush 1	46.0 ± 0.86	72.51 ± 1.56	1177 ± 76.1	550.0 ± 7.1	0.98 ± 0.05	125.2 ± 3.6	27.7 ± 0.10
Crush 2	69.0 ± 1.26	102.92 ± 2.38	1617 ± 90.5	584.0 ± 7.4	0.94 ± 0.06	194.6 ± 5.3	44.9 ± 0.16
Crush 3	36.1 ± 0.66	50.84 ± 1.04	813.0 ± 45.4	227.4 ± 2.6	0.31 ± 0.05	81.4 ± 2.4	35.6 ± 0.11
Crush 4	17.9 ± 0.28	25.64 ± 0.52	403.7 ± 23.0	97.4 ± 0.58	0.08 ± 0.05	7.0 ± 0.6	9.00 ± 0.05
Heating							
200°C	5.1 ± 0.21	0.78 ± 0.18	20.0 ± 25.7				
400°C	40.1 ± 1.70	17.22 ± 2.26	194.4 ± 11.8				
600°C	25.3 ± 1.04	31.01 ± 4.08	267.6 ± 18.2				
800°C	7.74 ± 0.32	8.99 ± 1.17	141.4 ± 10.4				
1000°C	5.04 ± 0.08	5.53 ± 0.32	83.2 ± 16.1				
1200°C	23.1 ± 0.34	25.88 ± 1.56					
1400°C	41.1 ± 0.61	45.39 ± 2.76	60.3 ± 151.1				
Total	316.4 ± 2.73	386.3 ± 6.54	4778 ± 202				
BC5-B							
Crush 1	137.6 ± 2.55	234.30 ± 12.6	3829 ± 216.7	1137 ± 14.4	2.78 ± 0.06	82.2 ± 2.48	7.20 ± 0.03
Crush 2	40.2 ± 0.62	69.01 ± 1.50	1196 ± 67.2	246.9 ± 1.33	0.59 ± 0.04	15.3 ± 0.51	1.37 ± 0.03
Crush 3	69.3 ± 1.06	125.37 ± 2.61	2207 ± 123	227.9 ± 1.21	0.40 ± 0.05	12.4 ± 0.60	2.41 ± 0.02
Crush 4	34.1 ± 0.55	54.01 ± 1.42	907.8 ± 51.3	97.9 ± 0.52	0.14 ± 0.06	5.40 ± 0.18	1.13 ± 0.02
Heating							
400°C	91.7 ± 1.43	30.82 ± 0.40	286.8 ± 34.6				
600°C	46.7 ± 0.71	55.35 ± 1.26	806.3 ± 45.7				
800°C	10.1 ± 0.16	14.52 ± 0.19	249.6 ± 14.2				
1000°C	6.83 ± 0.12	7.50 ± 0.21	122.6 ± 7.02				
1200°C	35.2 ± 0.53	42.03 ± 1.14	618.6 ± 54.3				
1400°C	43.4 ± 0.72	52.11 ± 0.65	788.6 ± 45.8				
Total	*515.1 ± 3.42*	*684.6 ± 13.2*	*11012 ± 279*				
BC5-C							
Crush 1	25.0 ± 0.38	49.48 ± 1.02	739.5 ± 41.0	567.0 ± 3.17	1.35 ± 0.04	39.0 ± 1.03	2.21 ± 0.03
Crush 2	248.9 ± 3.81	213.5 ± 11.0	6290 ± 359	2235 ± 11.9	3.84 ± 0.04	132.3 ± 4.19	7.38 ± 0.05
Crush 3	96.0 ± 1.49	155.7 ± 3.34	2284 ± 128	570.5 ± 4.36	0.64 ± 0.07	20.0 ± 0.60	2.19 ± 0.03
Crush 4	77.5 ± 1.23	125.53 ± 12.6	1901 ± 104	407.2 ± 3.75	0.21 ± 0.04	9.37 ± 0.57	0.99 ± 0.02
Crush 5	84.5 ± 1.30	125.13 ± 2.69	1893 ± 105	397.0 ± 2.21	0.24 ± 0.05	7.36 ± 0.33	1.25 ± 0.05
Crush 6	37.6 ± 0.57	51.42 ± 1.07	793.2 ± 43.5	154.3 ± 0.86	0.09 ± 0.06	3.39 ± 0.28	1.03 ± 0.01
Heating							
400°C	157.5 ± 2.36	43.61 ± 1.51	419.5 ± 29.5				
600°C	66.6 ± 0.99	69.45 ± 1.65	953.4 ± 80.3				
800°C	13.4 ± 0.22	14.97 ± 0.43	226.4 ± 12.5				
1000°C	11.5 ± 0.18	11.82 ± 0.47	143.6 ± 16.1				
1200°C	76.5 ± 1.17	86.34 ± 2.25	1373 ± 74.9				
1400°C	55.8 ± 0.84	51.92 ± 1.31	760.6 ± 41.8				
Total	*950.6 ± 5.39*	*998.4 ± 17.7*	*17778 ± 432*				
BC4							
Crush 1	8.34 ± 0.16	13.31 ± 0.12	188.4 ± 5.88	306.6 ± 3.68	0.58 ± 0.03	33.7 ± 0.44	4.36 ± 0.01
Crush 2	16.5 ± 0.31	27.33 ± 0.24	359.4 ± 9.81	423.8 ± 5.07	0.56 ± 0.04	20.1 ± 0.29	2.19 ± 0.00
Crush 3	13.4 ± 0.20	22.84 ± 0.26	318.8 ± 8.47	247.6 ± 0.72	0.30 ± 0.02	5.68 ± 0.30	0.76 ± 0.00
Crush 4	15.5 ± 0.23	28.96 ± 0.32	441.7 ± 11.9	209.3 ± 0.58	0.17 ± 0.04	3.94 ± 0.08	1.00 ± 0.00
Crush 5	19.0 ± 0.28	34.78 ± 0.36	490.2 ± 14.6	224.7 ± 0.74	0.23 ± 0.05	4.04 ± 0.25	1.37 ± 0.00
Crush 6	5.54 ± 0.09	9.28 ± 0.09	143.4 ± 4.26	76.0 ± 0.18	0.15 ± 0.04	1.66 ± 0.13	0.54 ± 0.01
Heating							
200°C	4.28 ± 0.06	0.67 ± 0.02	30.9 ± 1.01				
400°C	14.7 ± 0.22	13.93 ± 0.10	165.5 ± 2.5				
600°C	2.23 ± 0.03	3.04 ± 0.03	1.4 ± 3.3				
800°C	2.17 ± 0.05	2.42 ± 0.07	29.9 ± 3.1				
1000°C	2.93 ± 0.06	3.64 ± 0.03	45.2 ± 2.1				
1200°C	17.6 ± 0.26	26.17 ± 0.19	364.1 ± 7.1				
1400°C	11.3 ± 0.18	13.05 ± 0.09	175.1 ± 3.7				
1600°C	2.53 ± 0.04	10.02 ± 0.08	184.8 ± 3.8				
Total	*136.0 ± 0.68*	*209.0 ± 0.67*	*2939 ± 26.2*				
BC-3							
Crush 1	0.98 ± 0.03	2.61 ± 0.03	39.5 ± 2.60	18.9 ± 0.07	0.10 ± 0.03	1.70 ± 0.11	2.19 ± 0.01
Crush 2	7.97 ± 0.12	19.5 ± 0.21	323.1 ± 20.7	100.0 ± 0.27	0.23 ± 0.04	7.58 ± 0.17	6.92 ± 0.03
Crush 3	15.3 ± 0.23	37.9 ± 0.41	617.7 ± 39.8	157.6 ± 0.46	0.34 ± 0.04	9.57 ± 0.20	8.58 ± 0.05
Crush 4	15.4 ± 0.23	37.3 ± 0.40	602.9 ± 38.3	145.5 ± 0.45	0.23 ± 0.05	8.30 ± 0.14	5.36 ± 0.02
Crush 5	8.39 ± 0.16	17.8 ± 0.16	258.3 ± 6.27	82.8 ± 0.99	0.19 ± 0.03	5.72 ± 0.12	1.70 ± 0..01
Crush 6	8.43 ± 0.17	16.7 ± 0.15	244.6 ± 6.39	84.4 ± 1.02	0.18 ± 0.03	6.62 ± 0.10	2.36 ± 0.00

Table (Continued)

APPENDIX 1 (Continued)

Sample	Cl mol ($\times 10^{-9}$)	Br mol ($\times 10^{-12}$)	I mol ($\times 10^{-15}$)	^{40}Ar mol ($\times 10^{-15}$	^{36}Ar mol ($\times 10^{-15}$)	^{84}Kr mol ($\times 10^{-18}$)	^{129}Xe mol ($\times 10^{-18}$)
Heating							
200°C	6.79 ± 0.11	1.59 ± 0.02	27.7 ± 1.99				
400°C	15.0 ± 0.24	9.91 ± 0.08	87.9 ± 1.84				
600°C	1.85 ± 0.03	3.06 ± 0.10					
800°C	1.99 ± 0.09	3.73 ± 0.04					
1000°C	3.22 ± 0.06	5.23 ± 0.03					
1200°C	11.4 ± 0.17	20.1 ± 0.11	269.8 ± 4.10				
1400°C	8.31 ± 0.13	13.0 ± 0.08	170.7 ± 2.49				
1600°C	2.05 ± 0.03	11.0 ± 0.05	188.7 ± 3.33				
Total	*107.1 ± 0.55*	*199.4 ± 0.68*	*2831 ± 60.1*				
BC-2							
Crush 1	0.63 ± 0.02	1.33 ± 0.02	38.9 ± 1.82	284.9 ± 0.81	0.98 ± 0.04	26.9 ± 0.42	2.22 ± 0.01
Crush 2	0.88 ± 0.03	1.83 ± 0.01	50.1 ± 1.49	352.4 ± 1.26	1.15 ± 0.06	32.4 ± 0.32	1.98 ± 0.00
Crush 3	2.77 ± 0.05	5.76 ± 0.04	132.7 ± 3.16	651.3 ± 3.71	2.03 ± 0.03	58.0 ± 0.46	3.29 ± 0.01
Crush 4	4.10 ± 0.08	7.85 ± 0.05	187.7 ± 4.69	498.3 ± 4.21	1.56 ± 0.05	41.3 ± 0.42	2.59 ± 0.01
Crush 5	3.59 ± 0.06	6.74 ± 0.05	160.4 ± 3.99	289.6 ± 1.70	0.83 ± 0.04	21.3 ± 0.19	1.67 ± 0.00
Crush 6	2.20 ± 0.04	3.74 ± 0.02	85.9 ± 5.01	156.9 ± 0.89	0.44 ± 0.03	10.1 ± 0.14	0.87 ± 0.01
Crush 7	0.77 ± 0.02	1.26 ± 0.01	25.4 ± 1.77	50.2 ± 0.13	0.17 ± 0.04	3.27 ± 0.08	0.46 ± 0.00
Heating							
200°C	0.61 ± 0.05	0.26 ± 0.04					
400°C	2.31 ± 0.04	1.35 ± 0.05					
600°C	8.43 ± 0.15	0.06 ± 0.39					
800°C	6.65 ± 0.11	1.05 ± 0.11					
1000°C	7.09 ± 0.10	9.01 ± 0.06					
1200°C	2.68 ± 0.05	5.24 ± 0.03					
1400°C	1.33 ± 0.02	5.47 ± 0.03					
1600°C	0.07 ± 0.02	0.63 ± 0.02					
Total	*44.1 ± 0.26*	*51.6 ± 0.43*	*681.1 ± 9.04*				

Sample	Cl mol ($\times 10^{-9}$)	Br mol ($\times 10^{-12}$)	I mol ($\times 10^{-15}$)	^{40}Ar mol ($\times 10^{-15}$	^{36}Ar mol ($\times 10^{-15}$)	^{84}Kr mol ($\times 10^{-18}$)
SB8						
Crush 1	7.01 ± 0.11	10.6 ± 0.06	675.1 ± 21.2	332.3 ± 0.94	0.39 ± 0.03	11.33 ± 0.26
Crush 2	6.14 ± 0.09	8.44 ± 0.06	508.5 ± 16.0	286.2 ± 0.76	0.28 ± 0.05	9.12 ± 0.18
Crush 3	4.66 ± 0.07	7.02 ± 0.07	435.3 ± 14.4	271.9 ± 0.84	0.45 ± 0.05	9.70 ± 0.37
Crush 4	11.3 ± 0.17	16.7 ± 0.06	1081 ± 33.8	475.8 ± 1.17	0.41 ± 0.04	13.6 ± 0.30
Crush 5	7.38 ± 0.12	11.5 ± 0.09	718.2 ± 25.7	320.5 ± 0.87	0.28 ± 0.03	9.95 ± 0.23
Heating						
200°C	0.21 ± 0.02	0.36 ± 0.02	49.9 ± 3.59			
400°C	6.48 ± 0.11	8.87 ± 0.33	634.3 ± 44.0			
600°C	4.46 ± 0.10	7.53 ± 0.11	588.3 ± 34.8			
800°C	0.96 ± 0.04	1.95 ± 0.02	383.0 ± 31.9			
1000°C	1.76 ± 0.06	1.87 ± 0.12	1596 ± 117			
1200°C	13.0 ± 0.22	15.3 ± 0.53	1529 ± 92.3			
1400°C	9.26 ± 0.15	9.55 ± 0.44	542.4 ± 33.4			
1600°C	3.04 ± 0.06	9.71 ± 0.32	412.2 ± 26.5			
Total	*75.6 ± 0.4*	*109.4 ± 0.86*	*9152 ± 175.9*			
SB6						
Crush 1	5.96 ± 0.09	9.87 ± 0.05	671.8 ± 21.2	522.2 ± 1.06	1.42 ± 0.04	28.22 ± 0.54
Crush 2	8.57 ± 0.13	14.4 ± 0.06	931.2 ± 31.6	372.1 ± 0.81	0.75 ± 0.07	18.30 ± 0.23
Crush 3	8.21 ± 0.12	14.1 ± 0.09	924.0 ± 36.0	334.4 ± 0.67	0.68 ± 0.06	17.32 ± 0.26
Crush 4	7.68 ± 0.12	12.9 ± 0.06	828.5 ± 27.2	266.3 ± 0.86	0.52 ± 0.04	12.18 ± 0.22
Crush 5	7.50 ± 0.13	12.3 ± 0.10	775.9 ± 26.3	241.8 ± 0.52	0.40 ± 0.06	10.11 ± 0.13
Heating						
200°C	0.15 ± 0.03	0.19 ± 0.06	18.9 ± 1.39			
400°C	2.92 ± 0.06	4.97 ± 0.18	362.5 ± 23.9			
600°C	1.55 ± 0.04	2.40 ± 0.17	167.4 ± 11.3			
800°C	0.46 ± 0.03	0.44 ± 0.02	29.5 ± 2.54			
1000°C	1.19 ± 0.05	1.47 ± 0.04	93.6 ± 6.24			
1200°C	12.8 ± 0.23	14.7 ± 0.71	925.2 ± 56.9			
1400°C	10.5 ± 0.19	10.4 ± 0.13	431.8 ± 26.0			
1600°C	12.2 ± 0.24	27.5 ± 0.84	956.5 ± 65.1			
Total	*79.7 ± 0.48*	*125.6 ± 1.15*	*7117 ± 114.3*			
SB4						
Crush 1	12.0 ± 0.18	17.0 ± 0.15	1252 ± 41.6	1809 ± 4.84	5.36 ± 0.05	100.7 ± 0.60

Table (Continued)

APPENDIX 1 (Continued)

Sample	Cl mol ($\times 10^{-9}$)	Br mol ($\times 10^{-12}$)	I mol ($\times 10^{-15}$)	^{40}Ar mol ($\times 10^{-15}$	^{36}Ar mol ($\times 10^{-15}$)	^{84}Kr mol ($\times 10^{-18}$)
Crush 2	7.53 ± 0.13	9.75 ± 0.07	620.1 ± 21.7	967.0 ± 2.65	2.84 ± 0.06	47.8 ± 0.42
Crush 3	11.2 ± 0.17	15.7 ± 0.07	1090 ± 33.9	1029 ± 2.57	2.76 ± 0.05	55.0 ± 0.50
Crush 4	6.08 ± 0.12	8.56 ± 0.04	589.7 ± 19.5	444.5 ± 1.16	1.12 ± 0.04	23.0 ± 0.48
Heating						
200°C	0.51 ± 0.09	0.60 ± 0.06	527.1 ± 32.2			
400°C	9.59 ± 0.38	14.6 ± 0.34	2078 ± 131.5			
600°C	4.28 ± 0.16	7.37 ± 0.20	688.6 ± 41.2			
800°C	0.53 ± 0.03	0.50 ± 0.01	219.1 ± 15.4			
1000°C	1.20 ± 0.05	0.78 ± 0.01	292.3 ± 18.4			
1200°C	10.7 ± 0.16	8.4 ± 0.18	668.5 ± 40.4			
1400°C	25.3 ± 0.37	18.1 ± 0.70	846.1 ± 50.9			
1600°C	8.73 ± 0.13	18.4 ± 0.68	798.0 ± 47.7			
Total	*97.6 ± 0.68*	*119.9 ± 1.09*	*9670 ± 175.6*			
SB1						
Crush 1	1.93 ± 0.03			264.8 ± 0.52	0.77 ± 0.04	
Crush 2	3.36 ± 0.05			1026 ± 3.24	3.30 ± 0.06	
Crush 3	2.61 ± 0.05			681.3 ± 1.13	2.24 ± 0.05	
Crush 4	2.32 ± 0.08	0.75 ± 0.03		595.9 ± 0.90	1.92 ± 0.04	1.34 ± 2.15
Crush 5	2.15 ± 0.05	3.43 ± 0.02	196.3 ± 7.46	338.1 ± 0.56	1.06 ± 0.06	21.9 ± 0.45
Crush 6	1.70 ± 0.04	2.57 ± 0.02	140.8 ± 5.27	240.0 ± 0.60	0.74 ± 0.04	15.5 ± 0.24
Heating						
200°C	0.32 ± 0.02	0.72 ± 0.05	86.6 ± 7.83			
400°C	3.84 ± 0.06	4.84 ± 0.05	295.3 ± 17.4			
600°C	3.54 ± 0.06	3.12 ± 0.12	196.1 ± 11.9			
800°C	1.65 ± 0.04	0.38 ± 0.13				
1000°C	1.66 ± 0.03	1.05 ± 0.02	27.5 ± 1.96			
1200°C	8.53 ± 0.13	7.16 ± 0.08	380.0 ± 22.3			
1400°C	11.1 ± 0.16	9.88 ± 0.49	399.6 ± 57.8			
1600°C	4.47 ± 0.07	15.3 ± 0.72	858.0 ± 122.9			
Total	*49.17 ± 0.28*	*49.2 ± 0.90*	*2580 ± 139.7*			
GM3						
Crush 1	9.26 ± 0.15	8.80 ± 0.08	353.1 ± 12.0	1263.0 ± 2.20	2.49 ± 0.04	66.8 ± 0.72
Crush 2	7.69 ± 0.13	7.49 ± 0.04		822.8 ± 1.81	1.15 ± 0.05	33.1 ± 0.75
Crush 3	8.31 ± 0.13	7.93 ± 0.05	243.9 ± 8.33	773.3 ± 1.48	0.94 ± 0.05	26.3 ± 0.24
Crush 4	2.74 ± 0.06	2.70 ± 0.02	83.7 ± 3.40	245.5 ± 0.50	0.33 ± 0.06	7.7 ± 0.35
Heating						
200°C	0.13 ± 0.02	0.09 ± 0.01	6.28 ± 0.98			
400°C	1.54 ± 0.04	1.33 ± 0.07	34.4 ± 5.02			
600°C	1.36 ± 0.04	1.06 ± 0.06	27.1 ± 3.88			
800°C	0.16 ± 0.03	0.16 ± 0.01	5.51 ± 0.79			
1000°C	0.24 ± 0.02	0.39 ± 0.02	12.1 ± 1.90			
1200°C	2.06 ± 0.03	1.79 ± 0.09	75.2 ± 10.9			
1400°C	1.44 ± 0.04	1.71 ± 0.09	95.2 ± 13.7			
1600°C	1.86 ± 0.03	3.36 ± 0.16	100.6 ± 14.6			
Total	36.8 ± 0.26	36.8 ± 0.25	1037 ± 28.1			
GM4						
Crush 1	46.4 ± 0.68	55.2 ± 0.37	923.3 ± 32.3	3395 ± 7.63	9.18 ± 0.06	249.8 ± 1.26
Crush 2	30.4 ± 0.46	19.5 ± 6.59	275.7 ± 9.476	893.2 ± 2.06	1.66 ± 0.03	49.2 ± 0.34
Crush 3	13.4 ± 0.20	15.8 ± 0.06	254.9 ± 9.11	384.9 ± 0.96	0.74 ± 0.05	20.1 ± 0.39
Crush 4	14.4 ± 0.22	17.2 ± 0.09	253.9 ± 9.33	372.3 ± 0.85	0.48 ± 0.05	16.0 ± 0.25
Crush 5	3.83 ± 0.10	4.4 ± 0.03	58.0 ± 3.96	95.4 ± 1.41	0.09 ± 0.05	3.71 ± 0.60
Heating						
200°C	0.67 ± 0.01	0.45 ± 0.02	101.8 ± 15.0			
400°C	9.88 ± 0.15	8.89 ± 0.47	147.8 ± 21.2			
600°C	6.00 ± 0.09	5.66 ± 0.30	121.3 ± 17.5			
800°C	1.35 ± 0.07	1.06 ± 0.06	13.7 ± 4.0			
1000°C	1.81 ± 0.05	1.29 ± 0.07				
1200°C	8.42 ± 0.13	5.04 ± 0.25	11.3 ± 3.0			
1400°C	11.3 ± 0.18	5.82 ± 0.28	70.4 ± 10.6			
1600°C	4.33 ± 0.07	11.4 ± 0.55	175.8 ± 25.2			
Total	*152.1 ± 0.93*	*151.6 ± 6.66*	*2408 ± 55.5*			
PV6						
Crush 1	6.16 ± 0.09	6.07 ± 0.04	177.8 ± 6.02	1903.0 ± 5.20	2.01 ± 0.04	54.8 ± 0.36
Crush 2	3.97 ± 0.07	4.25 ± 0.03	114.9 ± 4.03	1047.1 ± 3.24	0.59 ± 0.06	18.7 ± 0.41
Crush 3	1.49 ± 0.04	1.78 ± 0.01	53.1 ± 2.82	419.7 ± 1.15	0.20 ± 0.03	6.33 ± 0.44

Table (Continued)

APPENDIX 1 (Continued)

Sample	Cl mol ($\times 10^{-9}$)	Br mol ($\times 10^{-12}$)	I mol ($\times 10^{-15}$)	^{40}Ar mol ($\times 10^{-15}$	^{36}Ar mol ($\times 10^{-15}$)	^{84}Kr mol ($\times 10^{-18}$)
Crush 4	2.48 ± 0.04	3.00 ± 0.02	77.9 ± 2.95	688.7 ± 1.90	0.21 ± 0.06	8.95 ± 0.18
Crush 5	0.53 ± 0.04	0.60 ± 0.01	28.5 ± 1.66	143.7 ± 0.42	0.06 ± 0.05	2.74 ± 0.23
Heating						
200°C	0.06 ± 0.05	0.04 ± 0.01	2.5 ± 0.23			
400°C	1.33 ± 0.04	1.39 ± 0.04	37.2 ± 2.56			
600°C	1.27 ± 0.02	1.40 ± 0.05	28.4 ± 1.71			
800°C	0.10 ± 0.03	0.12 ± 0.03				
1000°C	0.18 ± 0.02	0.20 ± 0.05				
1200°C	1.03 ± 0.04	0.89 ± 0.04	2.61 ± 1.47			
1400°C	0.88 ± 0.03	0.51 ± 0.06				
1600°C	0.80 ± 0.03	1.53 ± 0.08				
Total	20.28 ± 0.16	21.8 ± 0.15	522.8 ± 9.14			
PV1						
Crush 1	3.14 ± 0.05	4.42 ± 0.03	97.4 ± 8.09	2199 ± 5.84	5.48 ± 0.06	113.8 ± 1.01
Crush 2	3.21 ± 0.06	4.14 ± 0.03	71.9 ± 2.41	1117 ± 2.30	2.18 ± 0.05	44.5 ± 0.37
Crush 3	2.09 ± 0.04	2.88 ± 0.02	44.7 ± 2.02	529.7 ± 1.20	0.71 ± 0.04	16.9 ± 0.27
Crush 4	2.42 ± 0.06	3.36 ± 0.03	58.1 ± 3.01	493.0 ± 1.02	0.50 ± 0.05	10.3 ± 0.32
Heating						
200°C	0.14 ± 0.03	0.11 ± 0.07	1.90 ± 6.82			
400°C	2.20 ± 0.24	3.75 ± 0.54				
600°C	0.72 ± 0.16	2.10 ± 0.05	48.8 ± 5.59			
800°C	0.14 ± 0.02	0.17 ± 0.02	8.85 ± 0.56			
1000°C	0.12 ± 0.02	0.18 ± 0.04	4.23 ± 0.97			
1200°C	1.57 ± 0.04	1.56 ± 0.06	31.9 ± 2.60			
1400°C	0.97 ± 0.04	0.78 ± 0.05	10.7 ± 1.72			
1600°C	1.72 ± 0.05	2.60 ± 0.06	18.9 ± 1.79			
Total	*18.4 ± 0.32*	*26.1 ± 0.56*	*397.4 ± 13.3*			
R1						
Crush 1	36.2 ± 0.54	36.4 ± 0.20	403.7 ± 12.7	1835 ± 10.0	4.50 ± 0.04	116.2 ± 34.8
Crush 2	28.8 ± 0.42	27.4 ± 0.22	260.6 ± 10.5	656.9 ± 1.1	1.08 ± 0.03	18.2 ± 5.40
Crush 3	25.6 ± 0.38	24.9 ± 0.08	252.3 ± 8.2	524.2 ± 0.9	0.75 ± 0.04	12.8 ± 3.82
Crush 4	9.02 ± 0.14	8.83 ± 0.04	74.7 ± 2.8	175.3 ± 0.3	0.24 ± 0.05	1.57 ± 0.48
Heating						
200°C	0.76 ± 0.03	0.37 ± 0.02	46.2 ± 6.6			
400°C	9.30 ± 0.14	6.22 ± 0.31	70.5 ± 10.2			
600°C	7.29 ± 0.11	5.91 ± 0.32	57.7 ± 8.5			
800°C	1.33 ± 0.03	1.13 ± 0.05	6.10 ± 3.2			
1000°C	1.43 ± 0.03	1.01 ± 0.05	12.0 ± 2.1			
1200°C	17.1 ± 0.25	9.69 ± 0.46	108.0 ± 15.6			
1400°C	17.1 ± 0.25	8.59 ± 0.41	113.7 ± 16.5			
1600°C	8.81 ± 0.13	10.4 ± 0.50	112.9 ± 16.4			
Total	*162.6 ± 0.90*	*140.8 ± 1.0*	*1518 ± 37.0*			
R3						
Crush 1	7.75 ± 0.12	7.53 ± 0.04	166.2 ± 8.20	2006.3 ± 3.93	5.58 ± 0.05	33.38 ± 10.04
Crush 2	4.89 ± 0.08	4.30 ± 0.04	101.9 ± 3.48	773.4 ± 1.17	1.92 ± 0.06	5.83 ± 1.78
Crush 3	5.84 ± 0.10	5.27 ± 0.02	103.5 ± 4.31	767.0 ± 1.60	1.74 ± 0.05	6.23 ± 1.87
Crush 4	4.93 ± 0.09	4.46 ± 0.03	78.4 ± 3.07	666.9 ± 1.12	1.53 ± 0.05	4.79 ± 1.37
Crush 5	3.72 ± 0.09	3.41 ± 0.05	85.2 ± 8.17	1395.9 ± 2.25	4.14 ± 0.04	8.27 ± 2.50
Crush 6	5.40 ± 0.08	4.40 ± 0.14	68.1 ± 5.77	810.8 ± 2.04	1.74 ± 0.05	6.06 ± 1.79
Crush 7			17.4 ± 4.71	40.0 ± 0.13		
Heating						
200°C	0.09 ± 0.02	0.17 ± 0.01	22.1 ± 3.20			
400°C	2.43 ± 0.04	2.63 ± 0.13	49.9 ± 7.48			
600°C	2.13 ± 0.05	2.39 ± 0.12	39.8 ± 5.74			
800°C	0.26 ± 0.03	0.23 ± 0.02				
1000°C	0.61 ± 0.01	0.43 ± 0.02				
1200°C	5.52 ± 0.08	4.11 ± 0.20	79.0 ± 11.4			
1400°C	6.54 ± 0.10	3.80 ± 0.18	80.8 ± 12.1			
1600°C	3.14 ± 0.05	5.46 ± 0.28	88.2 ± 12.8			
Total	*53.3 ± 0.28*	*48.6 ± 0.46*	*980.5 ± 27.7*			
M3						
Crush 1	2.75 ± 0.06	2.74 ± 0.03	88.5 ± 3.26	812.9 ± 2.29	2.70 ± 0.04	0.61 ± 0.02
Crush 2	6.29 ± 0.10	5.96 ± 0.03	184.7 ± 6.95	678.3 ± 1.66	2.13 ± 0.04	0.46 ± 0.01
Crush 3	4.37 ± 0.08	3.99 ± 0.03	125.6 ± 7.04	175.5 ± 0.88	0.54 ± 0.06	0.03 ± 0.01
Crush 4	3.14 ± 0.05	2.73 ± 0.02	80.4 ± 3.34	133.2 ± 0.53	0.43 ± 0.03	0.02 ± 0.01
Crush 5	2.70 ± 0.06	2.44 ± 0.02	65.1 ± 3.66	109.5 ± 0.42	0.35 ± 0.03	0.01 ± 0.01

Table (Continued)

APPENDIX 1 (Continued)

Sample	Cl mol ($\times 10^{-9}$)	Br mol ($\times 10^{-12}$)	I mol ($\times 10^{-15}$)	^{40}Ar mol ($\times 10^{-15}$	^{36}Ar mol ($\times 10^{-15}$)	^{84}Kr mol ($\times 10^{-18}$)
Heating						
200°C	0.18 ± 0.02	0.17 ± 0.03	21.6 ± 3.14			
400°C	1.99 ± 0.04	1.55 ± 0.09	52.4 ± 7.62			
600°C	1.87 ± 0.03	1.51 ± 0.08	50.1 ± 7.41			
800°C	0.87 ± 0.04	0.64 ± 0.03	8.69 ± 1.32			
1000°C	0.53 ± 0.02	0.44 ± 0.02				
1200°C	5.32 ± 0.08	3.42 ± 0.21	119.8 ± 17.7			
1400°C	7.18 ± 0.11	4.29 ± 0.23	153.1 ± 23.6			
1600°C	7.79 ± 0.12	6.96 ± 0.33	383.6 ± 55.0			
	0.28 ± 0.02	5.47 ± 0.35	553.7 ± 80.2			
Total	45.3 ± 0.25	42.3 ± 0.59	1887 ± 102.9			

Sample	^{3}He/^{4}He	^{40}Ar/^{36}Ar	^{40}Ar*/^{4}He ($\times 10^{-3}$)	^{20}Ne/^{36}Ar ($\times 10^{-3}$)
SB5	1.12 ± 0.01	913.8 ± 2.6	697.3 ± 0.8	325.0 ± 62.0
SB6	0.84 ± 0.02	924.1 ± 2.1	590.9 ± 0.6	666.8 ± 12.2
SB4	1.20 ± 0.01	852.2 ± 6.3	685.6 ± 0.9	396.7 ± 9.6
PV6(py)	0.62 ± 0.03	670.0 ± 3.8	1005.9 ± 1.2	460.2 ± 11.5
PV6(cpy)	0.76 ± 0.02	1063.1 ± 4.8	1325.9 ± 1.6	349.0 ± 3.8
PV1	1.15 ± 0.03	603.1 ± 1.8	1075.7 ± 2.4	797.3 ± 15.9
R3	1.72 ± 0.01	813.4 ± 1.8	972.0 ± 1.0	305.9 ± 2.6
R1	1.38 ± 0.06	547.4 ± 2.5	1755.5 ± 2.7	395.3 ± 2.1
GM3 (cpy)	0.32 ± 0.01	907.2 ± 1.1	366.6 ± 0.4	468.1 ± 2.5
GM3 (py)	0.60 ± 0.02	845.3 ± 21.8	612.1 ± 1.0	1187.7 ± 32.5